

NASA TECHNICAL NOTE



NASA TN D-7887

NASA TN D-7887

**CASE FILE
COPY**

**EFFECTS OF GEOMETRIC VARIABLES ON
THE PERFORMANCE OF A PROBE FOR
DIRECT MEASUREMENT OF FREE-STREAM
STAGNATION PRESSURE IN SUPERSONIC FLOW**

Lana M. Couch

*Langley Research Center
Hampton, Va. 23665*



1. Report No. NASA TN D-7887		2. Government Accession No.		3. Recipient's Catalog No.	
4. Title and Subtitle EFFECTS OF GEOMETRIC VARIABLES ON THE PERFORMANCE OF A PROBE FOR DIRECT MEASUREMENT OF FREE-STREAM STAGNATION PRESSURE IN SUPERSONIC FLOW				5. Report Date May 1975	
				6. Performing Organization Code	
7. Author(s) Lana M. Couch				8. Performing Organization Report No. L-9757	
9. Performing Organization Name and Address NASA Langley Research Center Hampton, Va. 23665				10. Work Unit No. 501-06-08-03	
				11. Contract or Grant No.	
12. Sponsoring Agency Name and Address National Aeronautics and Space Administration Washington, D.C. 20546				13. Type of Report and Period Covered Technical Note	
				14. Sponsoring Agency Code	
15. Supplementary Notes					
16. Abstract <p>An investigation was conducted at Mach numbers of 1.41, 1.83, and 2.20 to determine the effects of parametric variations in the height of the pitot-tube center line from the probe surface (achieved by varying the pitot-tube diameter) and in the radius of the surface curvature on the pressure recovery of a probe designed to measure the free-stream stagnation pressure. The probe consists of a pitot tube mounted on the surface of a curved cylinder of circular cross section; the pitot tube senses the pressure of the stream tube which has been slowed by isentropic compression along the curved surface. Pressure recovery, greater than or equal to 99.8 percent of the free-stream stagnation pressure, was obtained for a wide range both of angle of attack and of yaw for probes satisfying the optimum design criteria determined in this investigation.</p>					
17. Key Words (Suggested by Author(s)) Pressure probe Pressure Supersonic Stagnation pressure				18. Distribution Statement Unclassified - Unlimited New Subject Category 01	
19. Security Classif. (of this report) Unclassified		20. Security Classif. (of this page) Unclassified		21. No. of Pages 68	
				22. Price* \$4.25	

EFFECTS OF GEOMETRIC VARIABLES ON THE PERFORMANCE OF A
PROBE FOR DIRECT MEASUREMENT OF FREE-STREAM
STAGNATION PRESSURE IN SUPERSONIC FLOW

By Lana M. Couch
Langley Research Center

SUMMARY

A parametric study was conducted to determine the effects of geometric variations in a probe designed to measure free-stream stagnation pressure. The probe consists of a pitot tube mounted on the surface of a curved cylinder of circular cross section; the pitot tube senses the pressure of the stream tube which has been slowed by isentropic compression along the curved surface. The variable geometric parameters were the height of the pitot-tube center line above the probe surface (achieved by varying the pitot-tube diameter) and the radius of the curvature of the cylinder. The investigation was conducted in the Langley 4-foot supersonic pressure tunnel at Mach numbers of 1.41, 1.83, and 2.20 and at a free-stream stagnation pressure of 103.42 kPa. Some additional data were obtained at free-stream stagnation pressures of 68.95 and 137.90 kPa at a Mach number of 1.83.

Two general trends were observed for the probes tested at a constant Mach number either for increasing the height of the pitot-tube center line above the surface or for decreasing the radius of the curvature of the probe surface. The pressure recovery decreased at a constant angle of attack and the magnitude of the variation of the pressure recovery increased with an increasing angle of attack.

Increasing the Mach number from 1.41 to 2.20 generally resulted in a decrease in both the magnitude and width of the plateau of the maximum pressure recovery. However, optimum pressure recoveries were obtained for probes with the ratio of the height of the pitot-tube center line from the probe surface to the probe-shaft diameter no greater than about 0.079 and the ratio of the radius of the surface curvature to the probe-shaft diameter of about 5 or 6. For the probes satisfying these design criteria, the plateau of optimum pressure recovery, greater than 99.8 percent of the free-stream stagnation pressure, was maintained over an angle-of-attack range varying from approximately 31° in width at $M = 1.41$ to about 14° at $M = 2.20$. For the variation in angle of yaw, the width of the optimum pressure-recovery plateau varied from an average width of 17° at $M = 1.41$ to about 10° at $M = 2.20$.

Generally, varying the Reynolds number had a negligible effect on the magnitude or the plateau width of the pressure recovery obtained for probes with varying geometry, except for the probe with the smallest radius of surface curvature (a ratio of radius of surface curvature to probe-shaft diameter of 2). For this probe the pressure recovery decreased with a decreasing Reynolds number at high angles of attack.

INTRODUCTION

The inability to measure the stagnation pressure directly in supersonic flow results in a degree of uncertainty in the determination of supersonic flow conditions. The stagnation pressure is generally determined indirectly from measurements of pitot and static pressures and, as a result, contains some inaccuracy because of the difficulty in measuring static pressure. The wind-tunnel test results of references 1 and 2 have proven the concept of a probe designed by M. J. Goodyer (Brit. R.A.E.) which directly measures the free-stream stagnation pressure in supersonic flow. The probe consists of a pitot tube mounted on the surface of a curved cylinder of circular cross section; the pitot tube senses the pressure of the stream tube which has been slowed by isentropic compression along the curved surface.

A parametric study to determine the effects of variation both in the height of the pitot-tube center line above the probe surface (achieved by varying the pitot-tube diameter) and in the radius of the curvature of the surface, on the pressure recovery of a probe designed to measure free-stream stagnation pressure has been conducted in the Langley 4-foot supersonic-pressure tunnel. The data were obtained at Mach numbers of 1.41, 1.83, and 2.20 and at a free-stream stagnation pressure of 103.42 kPa over a range of angle of attack and of yaw. Some additional data were obtained at free-stream stagnation pressures of 68.95 and 137.90 kPa at a Mach number of 1.83.

SYMBOLS

D	diameter of probe shaft
d	inside diameter of pitot tube
M	free-stream Mach number
N_{Re}	Reynolds number
$p_{t,1}$	average free-stream stagnation pressure in the test section, corrected for stagnation-pressure losses between the settling chamber and the test section (based on the wind-tunnel calibration)

R	pressure recovery, equal to ratio of pressure measured by probe to local free-stream stagnation pressure
r	radius of surface curvature
y	height of pitot-tube center line from probe surface
α	angle of attack (see fig. 1)
β	angle of yaw (see fig. 1)

APPARATUS AND TESTS

Wind Tunnel

The investigation was conducted in the Langley 4-foot supersonic pressure tunnel at free-stream Mach numbers of 1.41, 1.83, and 2.20. This continuous-flow wind tunnel has a stagnation-pressure range from approximately 21.0 to 207.0 kPa at a stagnation temperature of 317.6 K. Discrete Mach numbers can be obtained from 1.41 to 2.20 by using interchangeable nozzle templates.

Probes and Support

Nine probes were tested as shown in figures 1 and 2: one series of five probes having different pitot-tube diameters (fig. 2(b)) and the other series of probes having different surface curvatures (fig. 2(c)). The pitot tubes of the first series ranged in inside diameter from 0.051 to 0.254 centimeter in increments of approximately 0.05 centimeter ($y/D = 0.053, 0.080, 0.120, 0.167, \text{ and } 0.167$). The radius of curvature of the compression surfaces of these five probes was 5.72 centimeters ($r/D = 6.0$). The other series of probes had compression surfaces with radii of curvature of 1.91, 2.86, 3.81, 4.76, and 5.72 centimeters ($r/D = 2, 3, 4, 5, \text{ and } 6$, respectively). The pitot tubes for these probes had a 0.051-centimeter inside diameter ($y/D = 0.053$). The probe having the $r/D = 6$ compression surface and the $y/D = 0.053$ pitot tube was incorporated as one of the probes for both series.

The probes were mounted on a spider support so that five models could be tested simultaneously, as shown in figure 2. The spider support was mounted in a remotely controlled pitching mechanism, which in conjunction with the permanent test-section strut allowed for online variation in both angle of attack and yaw. The probes and the spider support were constructed of 347 stainless steel. The face of each pitot tube was square with no chamfer, and each pitot tube was soldered in place against the compression sur-

face, as shown in figure 1. The surface distance of the pitot tube from the probe tip has been optimized in previous tests by this investigator; in addition, pertinent data on pitot-tube location are presented in reference 2.

Test Conditions

The major portion of the investigation was conducted at a free-stream stagnation pressure of 103.42 kPa at Mach numbers of 1.41, 1.83, and 2.20. Some additional data were obtained at free-stream stagnation pressures of 68.95 and 137.90 kPa at a Mach number of 1.83. The stagnation temperature was held constant at 317.6 K.

Corrections

Since five probes were tested simultaneously, each in a different position in the wind tunnel, one probe, identical in design to a probe which had been tested previously, was mounted in the center position of the spider support. This probe ($r/D = 6$ and $y/D = 0.053$) remained in the center position both for the test of the series of probes with varying pitot-tube size and for the series with varying surface curvature. Since some small variations in the free-stream stagnation pressure could exist at different locations in the test section and since the relative merits of the probes were to be compared, this probe was tested at each of the positions of the spider support throughout the complete Mach number, angle-of-attack, and angle-of-yaw ranges. The increment between the maximum recovery factor obtained and the recovery factor obtained at each other position with this same probe was added to the recovery factors obtained with each of the other probes according to their position on the support during testing. Therefore each of the probes was, in effect, tested in the same flow, since the use of this method accounted for the small variations in stagnation pressure that exist throughout a test section. The average correction to the recovery factor for the variation in stagnation pressure was approximately 0.00050.

Previous tests of a probe, similar in design to the probes of this investigation, had shown that significant losses in stagnation pressure were incurred because of condensation of the moisture in the airstream. Since any loss in stagnation pressure measured by the probes, relative to the settling-chamber stagnation pressure, would appear to be a deficiency in probe performance, a strong emphasis was placed on drying the airstream. The initial test run at each of the three test Mach numbers consisted of obtaining the variation of the probe total-pressure recovery with increasing drying of the airstream (decreasing dewpoint temperature). The airstream was dried until no further increases in the pressure recovery were obtained with a decreasing dewpoint temperature. The data were obtained continually during the drying procedure so that each data point obtained subsequently could be corrected for condensation losses. However, an attempt was made

throughout the investigation to keep the airstream as dry as possible in order to minimize the magnitude of the correction. The average correction to the recovery factor to account for condensation losses was approximately 0.00040. From this investigation it was determined that in this facility at Mach numbers of 1.41, 1.83, and 2.20, the airstream dried to dewpoint temperatures of 241.5 K, 234.8 K, and 230.4 K, respectively, is sufficiently dry so that further drying results in no increase in the probe stagnation-pressure recovery. Corrections to the data obtained at $M = 1.41$ were unnecessary, since all these data were obtained at dewpoint temperatures below 241.5 K. The data obtained at Mach numbers of 1.83 and 2.20 were corrected, where necessary, for condensation losses.

Instrumentation and Accuracy

The stagnation pressure in the settling chamber and the pressure for the center experimental probe were measured on precision mercury manometers, which had an accuracy level of ± 0.05 kPa. The pressures measured by the other four experimental probes were referenced to the pressure measured by the center-positioned probe and were measured with individual 3.45 kPa differential-pressure transducers (Accuracy level = ± 6.89 Pa) at Mach numbers of 1.41 and 1.83. At a Mach number of 2.20, individual 17.25-kPa differential-pressure transducers (Accuracy level = ± 0.021 kPa) were required in order to accommodate the pressure differential incurred in passing the shock wave through the test section. All the transducers were carefully selected, based on calibration results, in order to minimize inaccuracies.

The stagnation temperature was measured using an iron-constantan thermocouple. A thermoelectric hygrometer, which provides a continuous output of the dewpoint temperature from a thermistor (Accuracy = ± 0.56 K), was monitored, and the dewpoint temperature was recorded automatically at each data point. Therefore, as a result of the total possible inaccuracies in the pressures and the dewpoint temperature, the accuracy level of R is ± 0.0010 , ± 0.0012 , and ± 0.0016 at Mach numbers of 1.41, 1.83, and 2.20, respectively.

The angle of attack was measured by use of an accelerometer with an accuracy of $\pm 0.02^\circ$. The angle of yaw was measured with a variable-resistance potentiometer with an accuracy of $\pm 0.1^\circ$. The Mach number was accurate to ± 0.005 .

Schlieren photographs were obtained throughout the angle-of-attack range at Mach numbers of 1.83 and 2.20 for the series of probes with varying surface curvature.

RESULTS AND DISCUSSION

The ability of a probe to measure free-stream stagnation pressure directly in supersonic flow depends on isentropically eliminating the strong normal shock wave that occurs

at the pitot tube. The flow-field sketch in figure 3 shows that the sampled flow first traverses a distributed-compression fan which is generated by the curved surface and is gradually decelerated. The pressure is then sampled by the pitot tube.

The effects of variation in both angle of attack and degree of surface curvature can be seen in the schlieren photographs of figure 4. At $\alpha = 2^\circ$ in figures 4(a) and 4(b) ($M = 1.83$ and 2.20 , respectively), the distributed-compression fan on the curved surface of the center probe for both conditions would be expected to provide a smooth, continuous compression even though there is a weak shock wave just ahead of the pitot tube. However, at $\alpha = 18^\circ$ and $M = 2.20$, fairly strong shock waves can be seen on the curved surface and just ahead of the pitot tube on the center probe and the compression is no longer isentropic. Increasing the radius of the surface curvature from the smallest to the largest probe (r/D from 2.0 to 6.0) results mainly in a more gradual compression along the curved surface, as can be seen both in figures 4(a) and 4(b).

Effect of Varying y/D

The variation of the pressure recovery with angle of attack at Mach numbers of 1.41 , 1.83 , and 2.20 is presented in figure 5 for probes having an $r/D = 6$ and pitot tubes with y/D ranging from 0.053 to 0.167 . Since the maximum inaccuracy in the recovery factor for these data is ± 0.0016 , recovery factors of 0.998 or greater are accepted as satisfactory performance for these probes in measuring $p_{t,1}$.

It should be noted that the height of the pitot-tube center line is the dominant parameter in the choice of pitot-tube size for these probes, as shown by the data in figure 5. The two probes with $y/D = 0.167$ had pitot tubes with different inside diameters, but as a result of having the same outside diameters, the center lines of the tubes were the same height from the probe surface. This similarity resulted in essentially the same performance in pressure recovery for these two probes. The inconsistently larger wall thickness for the probe with $d/D = 0.213$ ($y/D = 0.167$) resulted from the unavailability, during construction, of a more desirable wall thickness. At a Mach number of 1.41 , the two probes with the smallest pitot tubes maintained a pressure recovery greater than 99.8 percent of the free-stream stagnation pressure for a plateau width in angle of attack of approximately 31° . Even the probe indicating the poorest performance ($y/D = 0.167$ and $d/D = 0.213$) maintained this large pressure recovery for a plateau width of approximately 15° . Although all of the probes indicated a pressure recovery of at least 99.8 percent of the free-stream stagnation pressure over some finite angle range at $M = 1.41$, an increase in the Mach number to 2.20 resulted in only the probes with the two smallest pitot tubes ($y/D = 0.053$ and 0.080) indicating a similar high level of pressure recovery. In figure 5(c), the plateau width at $M = 2.20$ for a pressure recovery greater than 0.998 of $p_{t,1}$ is approximately 14° which is about one-half of the plateau width at $M = 1.41$.

Therefore, in order to maintain a pressure recovery of 99.8 percent of the free-stream stagnation pressure over a Mach number range from 1.41 to 2.20, the ratio y/D must be no greater than about 0.080 for a probe configured similarly to the probes of this investigation. Further, it appears that for this probe design, a Mach number of 2.20 may be approaching the upper limit in Mach number for the plateau of high pressure recovery (i.e., greater than 0.998 of $p_{t,1}$) to be sufficiently wide to be useful. At a Mach number of 1.83 (fig. 5(b)) the plateaus for the two probes with the smallest pitot tubes are incomplete at large, positive angles of attack because of time restrictions while testing that phase of the investigation.

Three general trends can be observed from these data: (1) as the ratio y/D increases, at a constant angle of attack, the pressure recovery decreases; (2) as the ratio y/D increases, the sensitivity of the pressure recovery to angle of attack increases; and (3) increasing the Mach number from 1.41 to 2.20 produces an overall deterioration in performance for these probes.

The variation of the pressure recovery for the probes having different values of y/D with angle of yaw at discrete angles of attack is presented in figures 6, 7, and 8 for Mach numbers of 1.41, 1.83, and 2.20, respectively. It should be pointed out that there is a lack of symmetry about 0° yaw in the trend of the pressure recoveries for these probes; a similar effect was observed in the data of reference 2. The cause of this asymmetry is, as yet, unknown. The highest overall pressure recovery at each angle of attack and Mach number is attained by the probes having the two smallest ratios of y/D with the $y/D = 0.080$ probe generally having the widest plateau in angle of yaw. The average width of the plateau of a pressure recovery greater than 0.998 for this probe is approximately 17° for angles of attack from about -7.8° to 14.0° , at $M = 1.41$. For angles of attack greater than 14.0° , not only does the overall pressure-recovery level decrease somewhat, but a sharp local decrease in pressure recovery occurs at about -4° in yaw. At the higher, positive angles of attack ($\alpha \approx 16^\circ$), the probes having the larger values of y/D indicate higher pressure recoveries and wider plateaus in yaw than the probes having the smallest values of y/D . In figure 7, generally, the same trends with the variation in yaw as were observed in figure 6 at $M = 1.41$ are indicated for the angles of attack at $M = 1.83$; the main differences result from the narrower, high pressure-recovery plateau at $M = 1.83$. In figure 8, where $M = 2.20$, both the overall level of the pressure recovery and its variation with yaw are much more sensitive to changes in y/D . Only the probes with the two smallest values of y/D attain a level of pressure recovery of 0.998 at this Mach number. The average width of the high pressure-recovery plateau in yaw is approximately 10° for angles of attack from about -1.8° to 8.2° . At angles of attack less than -1.8° , the level of the pressure recovery has dropped below 0.998 for all of the probes and there is really no useful plateau even at the lower pressure recoveries. In general,

either of the probes with $y/D = 0.053$ or 0.080 performs well for Mach numbers through 2.20, with the probe having $y/D = 0.080$ indicating slightly higher pressure recoveries and wider plateaus over both the angle-of-attack and the angle-of-yaw ranges.

Effect of Varying Radius of Curvature

The variation of pressure recovery with angle of attack at Mach numbers of 1.41, 1.83, and 2.20 is presented in figure 9 for probes having a $y/D = 0.053$ and surface curvatures ranging from a radius of 1.91 to 5.72 centimeters (r/D from 2.0 to 6.0). Throughout this Mach number range the probes having surface curvatures of $r/D = 5$ and 6 maintain the highest levels of pressure recovery and have the widest plateaus for $R \geq 0.998$; the widths of the plateaus range from approximately 31° at $M = 1.41$ to about 12° at $M = 2.20$. At Mach numbers of 1.41 and 1.83, all of these probes perform well, both in pressure recovery and plateau width. However, at $M = 2.20$, the three probes with the smallest radii indicate either large local disturbances at various angles of attack (for example, probes with $r/D = 2$ and 4) or a narrower plateau (probe with $r/D = 3$) than for the two larger radius probes.

The variation of the pressure recovery of the probes for each radius of curvature with angle of yaw at discrete angles of attack is presented in figures 10, 11, and 12 for Mach numbers of 1.41, 1.83, and 2.20, respectively. Although at some angles of attack and Mach numbers (for example, fig. 10(c), where $M = 1.41$ and $\alpha \approx 0^\circ$) all of the probes perform equally well, the two probes with the largest radii ($r/D = 5$ and 6) generally maintain the highest levels of pressure recovery and the widest plateaus. The width of the plateau in yaw for a pressure recovery greater than 0.998 for the probe with an r/D of 5 is approximately 10° for $-11.8^\circ \leq \alpha \leq 14.1^\circ$ at $M = 1.41$. In figure 11, where $M = 1.83$, all of the probes perform well throughout the angle-of-yaw range for $\alpha \approx -5.6^\circ$. However, for an angle of attack of -7.7° , the pressure recovery is less than 0.998 for all of the probes (a result of the narrower, high pressure-recovery plateau with angle of attack at this Mach number, as shown previously in fig. 5(b)). In figure 12, where $M = 2.20$, the probe with the largest radius of curvature has both the highest overall pressure-recovery level and the widest plateau in yaw for the angle-of-attack range. The smaller probes perform well for some angles of attack, but generally the plateaus are relatively narrow and large localized disturbances in the pressure recovery occur. Therefore, the probe with an $r/D = 6$ shows the superior performance in the pressure-recovery level and the plateau width for the Mach number range from 1.41 to 2.20.

Effect of Varying Unit Reynolds Number

The effect of changing unit Reynolds number at $M = 1.83$ on the pressure recovery obtained for probes having different values of y/D is shown in figure 13 for the variation of the pressure recovery with angle of attack ($\beta \approx 0^\circ$), and is shown in figure 14 for the

variation of the pressure recovery with angle of yaw at discrete angles of attack. All the differences between the sets of varying Reynolds number data for these two figures are equal to or within the accuracy of these data. Therefore, for variation in the distance of the pitot-tube center line from the surface, there is apparently only a negligible effect of varying the Reynolds number.

The effect of changing unit Reynolds number at $M = 1.83$ on the pressure recovery obtained for probes with different radii of curvature is shown in figure 15 for the variation of the pressure recovery with angle of attack ($\beta \approx 0^\circ$) and is shown in figure 16 for the variation of the pressure recovery with angle of yaw at discrete angles of attack. Generally, all the differences between the sets of varying Reynolds number data for these two figures are essentially within the accuracy of the data, the variation of the pressure recovery at high angles of attack for the probe with $r/D = 2.0$, as shown in figure 15, being the exception. For angles of attack greater than 8° , it appears that the pressure recovery at a given angle of attack decreases with a decreasing unit Reynolds number. The effect is most pronounced for $r/D = 2.0$ probe, since it has a very high rate of curvature and, therefore, a very short surface length from the probe tip to the pitot tube.

Effect of Varying Mach Number

The effect of Mach number on the variation of the pressure recovery with angle of attack is presented in figure 17 for each of the probes having different values of y/D and in figure 18 for each of the probes with different surface curvatures. In figure 17, for probes with $y/D \geq 0.120$, increasing the Mach number from 1.41 to 2.20 generally results in a decrease in both the magnitude and the width of the plateau of the maximum pressure recovery. However, the probes with $y/D \leq 0.080$ proved to have a superior performance in this Mach number range, as has been seen in previous figures. Although increasing the Mach number results in a decrease in the width of the plateau of maximum pressure recovery, the plateau is sufficient in width to be useful and there is very little deterioration in the magnitude of the maximum pressure recovery.

In figure 18, for probes with different surface curvatures, increasing the Mach number generally resulted in a decrease in the width of the plateau of maximum pressure recovery (or a complete collapse of the plateau) and a decrease in the magnitude of the maximum pressure recovery. However, a superior performance is shown for the probes having radii of curvature of $r/D = 5$ and 6 , since increasing the Mach number resulted in essentially no deterioration in the maximum pressure recovery. Also, the resulting plateau of the maximum pressure recovery is sufficiently wide to provide a useful angle-of-attack range.

CONCLUDING REMARKS

A parametric study to determine the effects of variation both in the pitot-tube diameter and the radius of surface curvature on the pressure recovery of a probe designed to measure free-stream stagnation pressure has been conducted in the Langley 4-foot supersonic pressure tunnel at Mach numbers of 1.41, 1.83, and 2.20. The study was conducted at a free-stream stagnation pressure of 103.42 kPa. Some additional data were obtained at free-stream stagnation pressures of 68.95 and 137.90 kPa at a Mach number of 1.83.

Two general trends were observed for the probes tested at a constant Mach number either for increasing the diameter of the pitot tube (that is, the height of the pitot-tube center line from the probe surface), or for decreasing the radius of curvature of the probe surface. The pressure recovery decreased at a constant angle of attack and the magnitude of the variation of the pressure recovery increased with an increasing angle of attack.

Increasing the Mach number from 1.41 to 2.20 generally resulted in a decrease in both the magnitude and width of the plateau of the maximum pressure recovery. However, optimum pressure recoveries, greater than or equal to 99.8 percent of the free-stream stagnation pressure, were obtained over the Mach number range for probes having the ratio of the distance of the pitot-tube center line from the probe surface to the probe-shaft diameter no greater than about 0.080 and the ratio of the radius of surface curvature to the probe-shaft diameter of about 5 or 6. For the probes satisfying these design criteria, the plateau of optimum pressure recovery was maintained over an angle-of-attack range varying from approximately 31° in width at $M = 1.41$ to about 14° at $M = 2.20$. For the variation in angle of yaw, the average width of the optimum pressure-recovery plateau varied from about 17° at $M = 1.41$ to about 10° at $M = 2.20$.

Generally, varying the Reynolds number had a negligible effect on the magnitude or the plateau width of the pressure recovery obtained for probes with varying geometry, except for the probe with the smallest radius of surface curvature (a ratio of radius of surface curvature to probe-shaft diameter of 2). For this probe the pressure recovery decreased with a decreasing Reynolds number at high angles of attack.

Langley Research Center,
National Aeronautics and Space Administration,
Hampton, Va., February 10, 1975.

REFERENCES

1. Goodyer, M. J.: A New Probe for the Direct Measurement of Stagnation Pressure in Supersonic Flow. Tech. Rep. 73122, British R.A.E., Mar. 1974.
2. Mundell, A. R. G.: Tests on Probes Designed To Measure Stagnation Pressure Directly in a Supersonic Stream. Tech. Rep. 73123, British R.A.E., Oct. 1973. (Available from DDC as AD 917 440.)

Pitot-tube series					Surface-curvature series						
Pitot tube				Surface curvature		Pitot tube			Surface curvature		
ID, cm	OD, cm	d/D	y/D	r, cm	r/D	ID, cm	OD, cm	d/D	y/D	r, cm	r/D
.051	.102	.053	.053	5.72	6.0	.051	.102	.053	.053	1.91	2.0
.102	.152	.107	.080	→	→	→	→	→	→	2.86	3.0
.152	.229	.160	.120	→	→	→	→	→	→	3.81	4.0
.203	.318	.213	.167	→	→	→	→	→	→	4.76	5.0
.254	.318	.267	.167	→	→	→	→	→	→	5.72	6.0

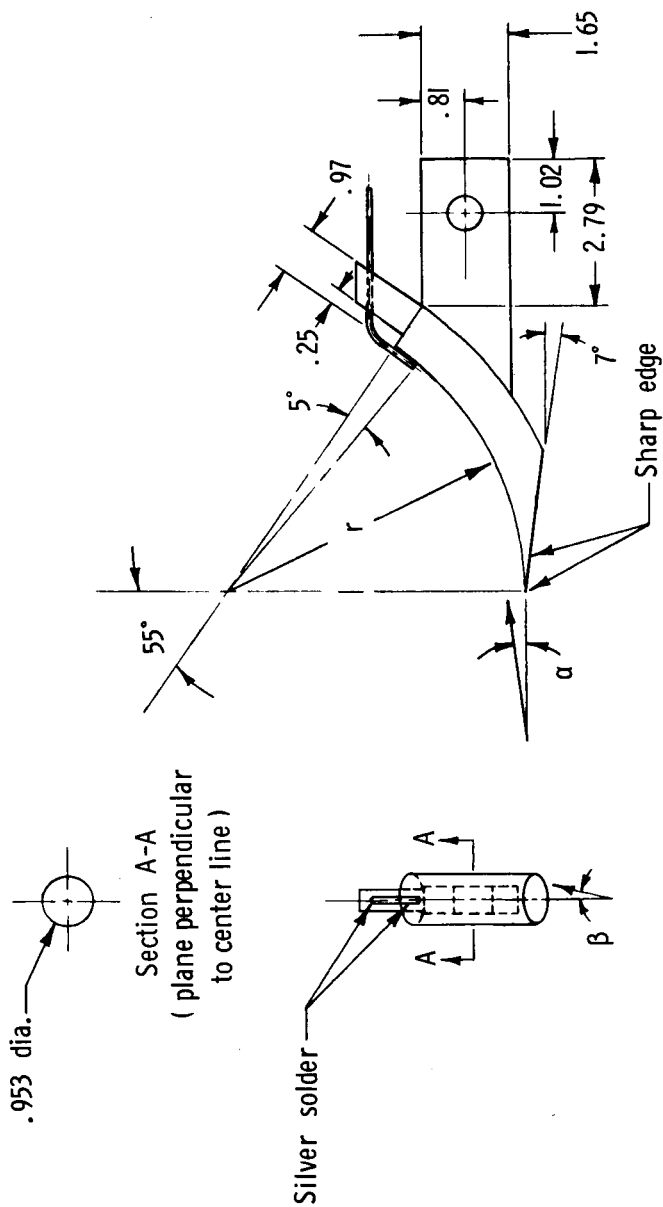
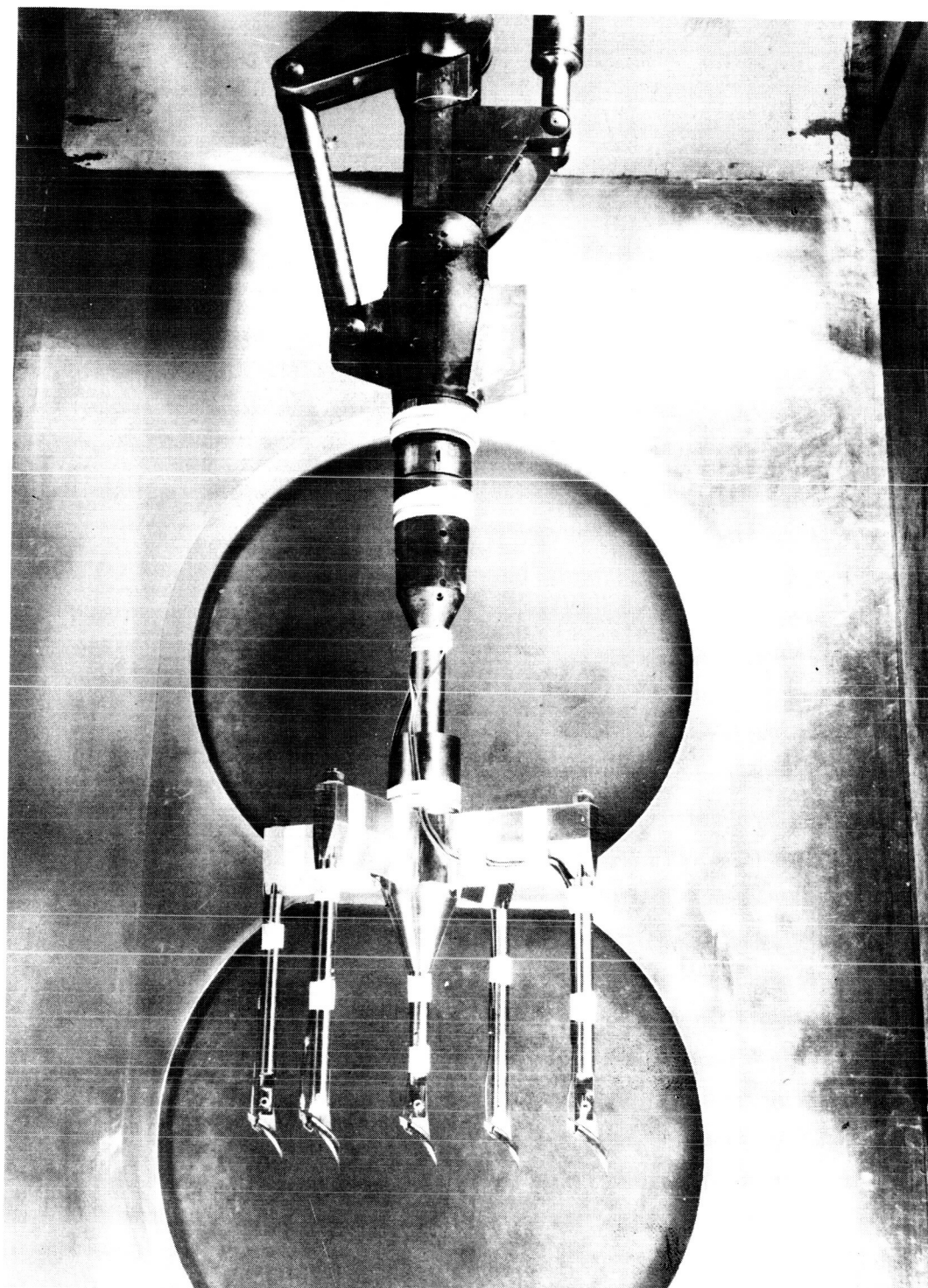


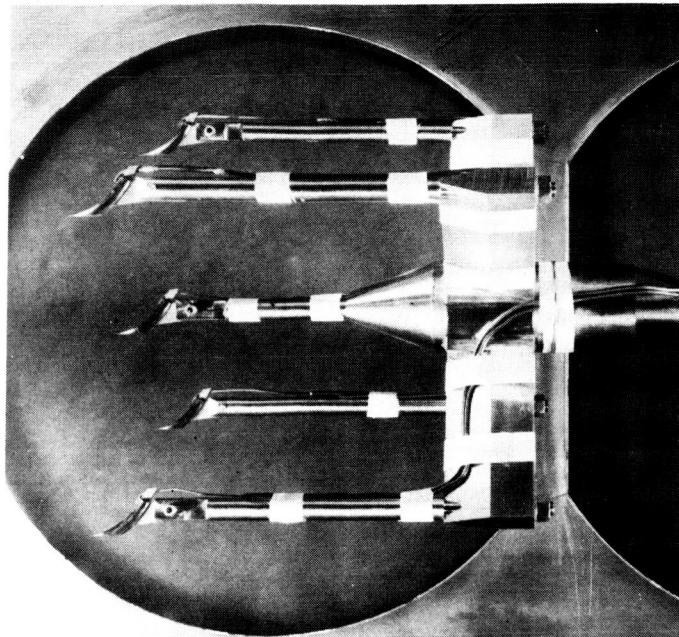
Figure 1.- General sketch of the probe. (All dimensions are in centimeters, unless otherwise noted.)



L-73-3747

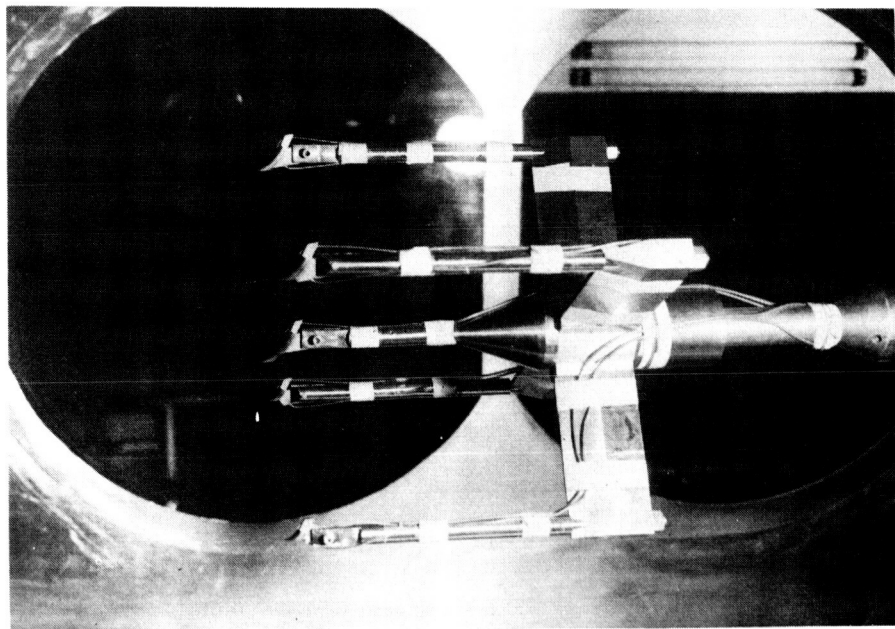
(a) Installation.

Figure 2.- Test probes.



L-73-3749

(b) Probes with different internal-diameter pitot tubes.



L-73-3946

(c) Probes with different surface curvatures.

Figure 2.- Concluded.

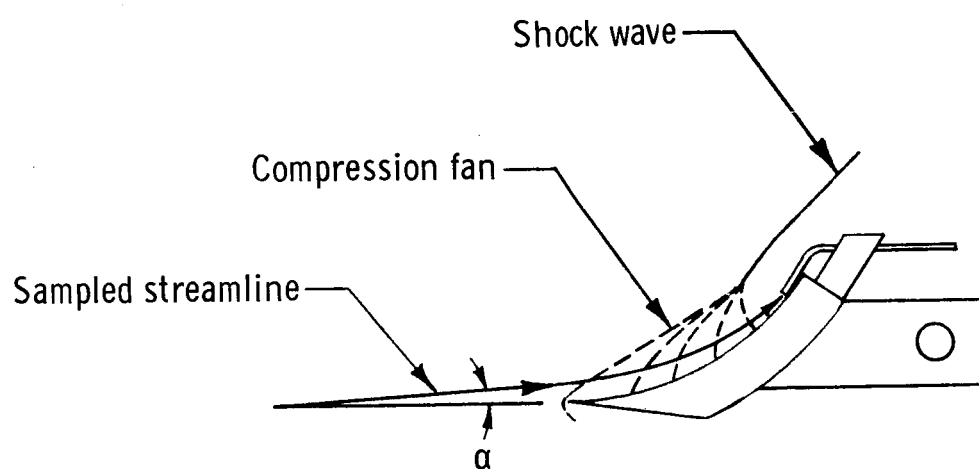
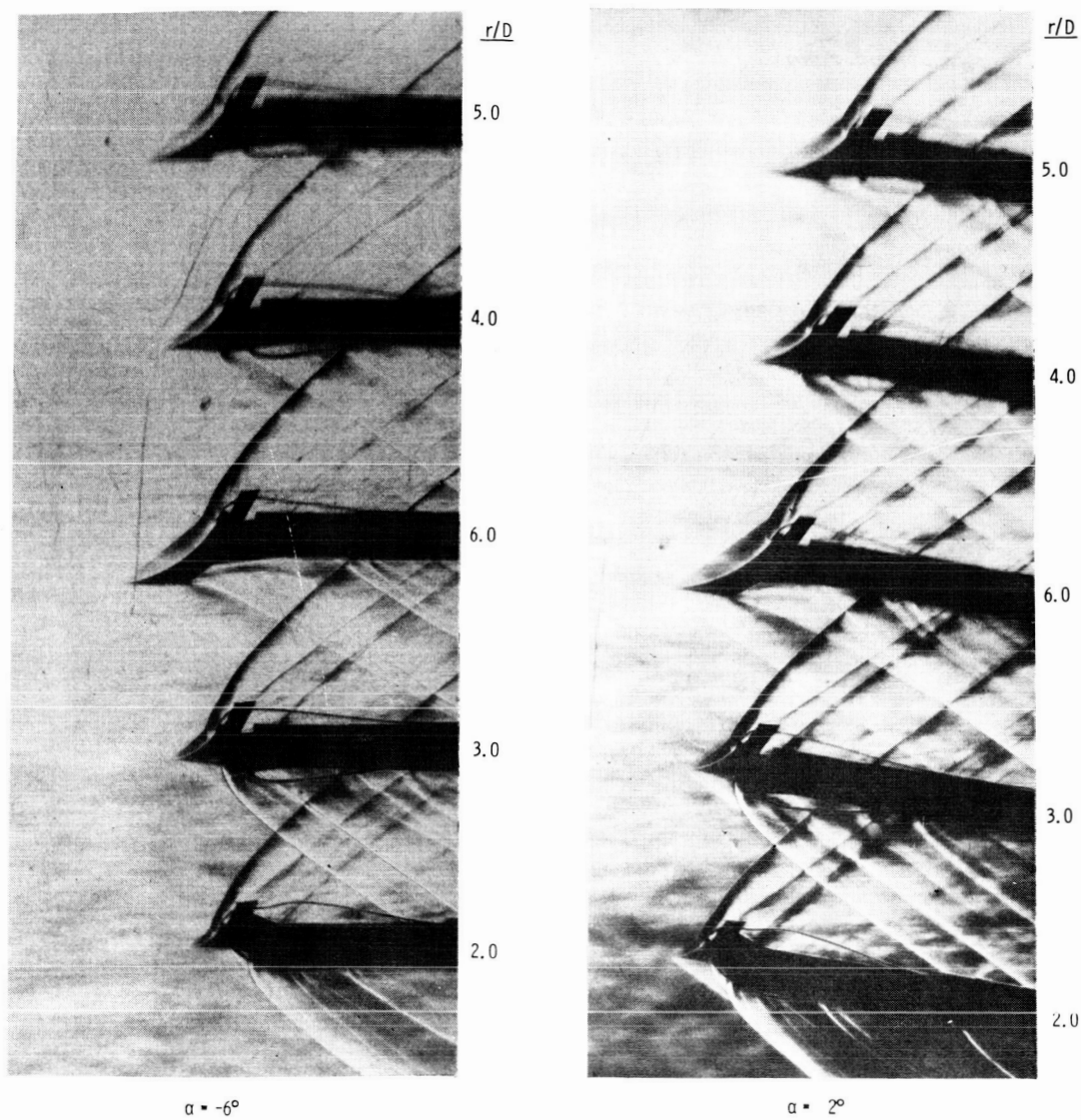


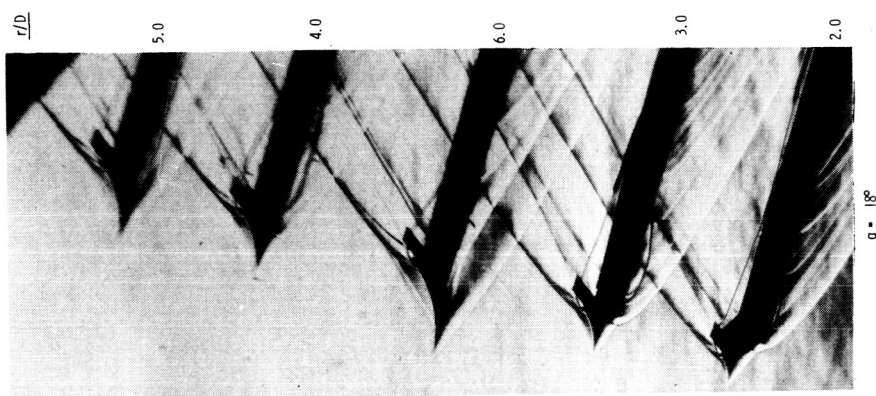
Figure 3.- Flow-field sketch.



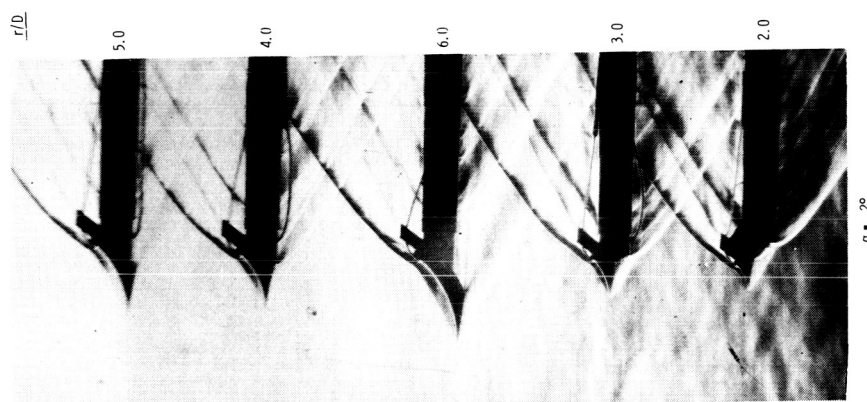
(a) $M = 1.83$.

L-75-143

Figure 4.- Schlieren photographs of probes with different surface curvatures.
 $y/D = 0.053$; $\beta \approx 0^\circ$.



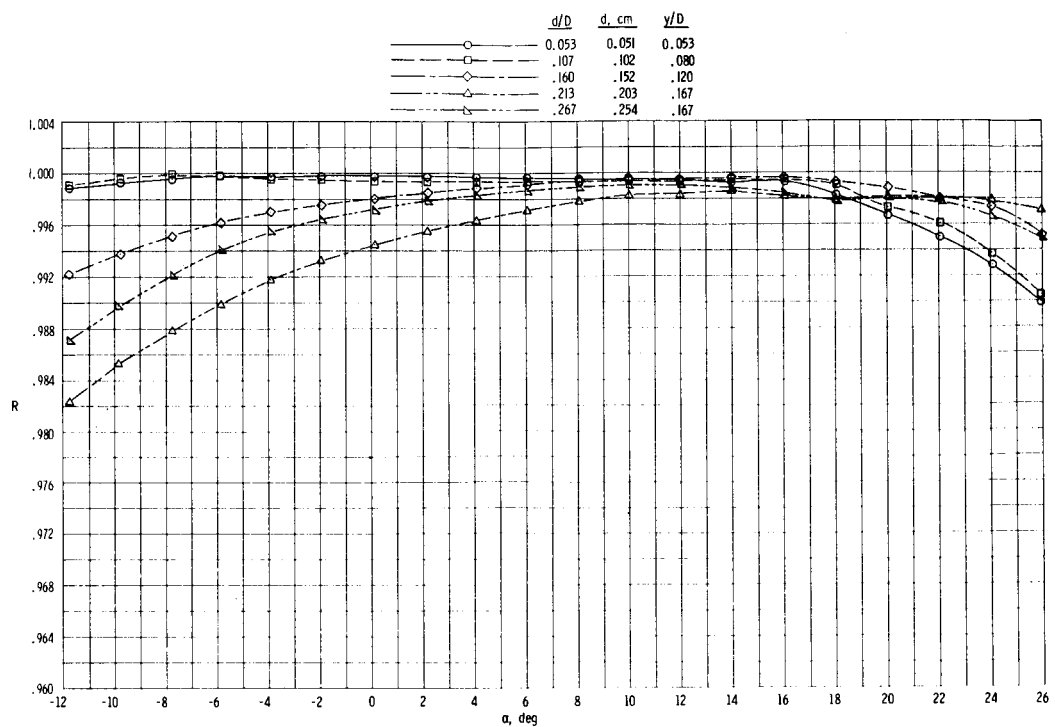
L-75-144



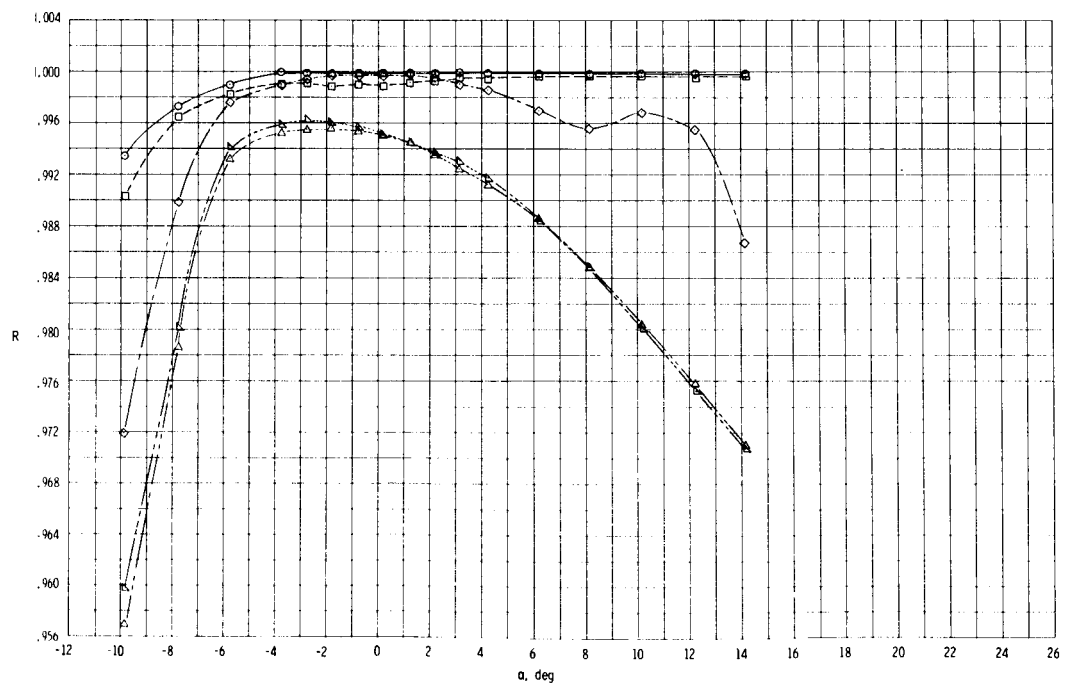
(b) $M = 2.20$.

Figure 4.- Concluded.



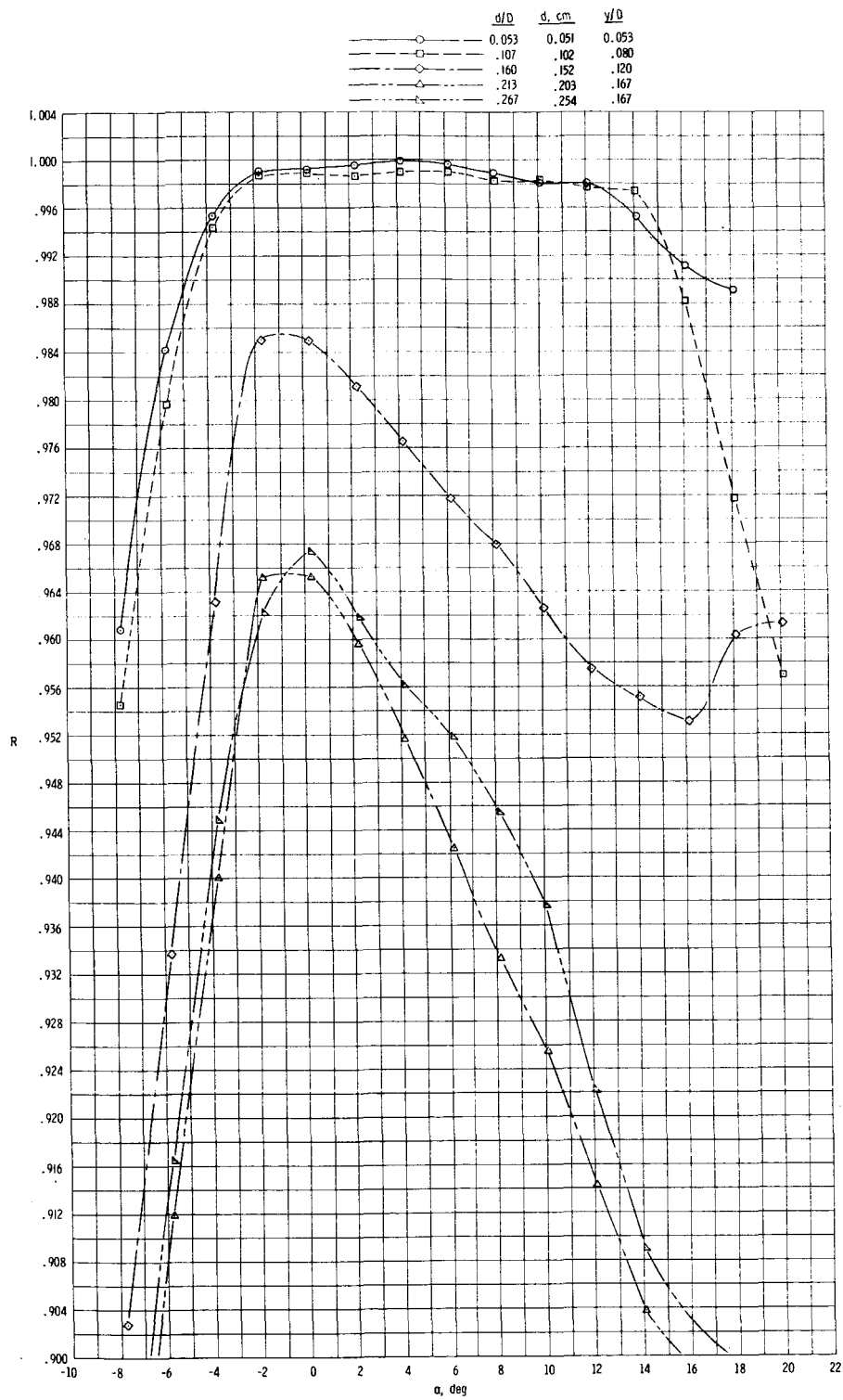


(a) $M = 1.41$.



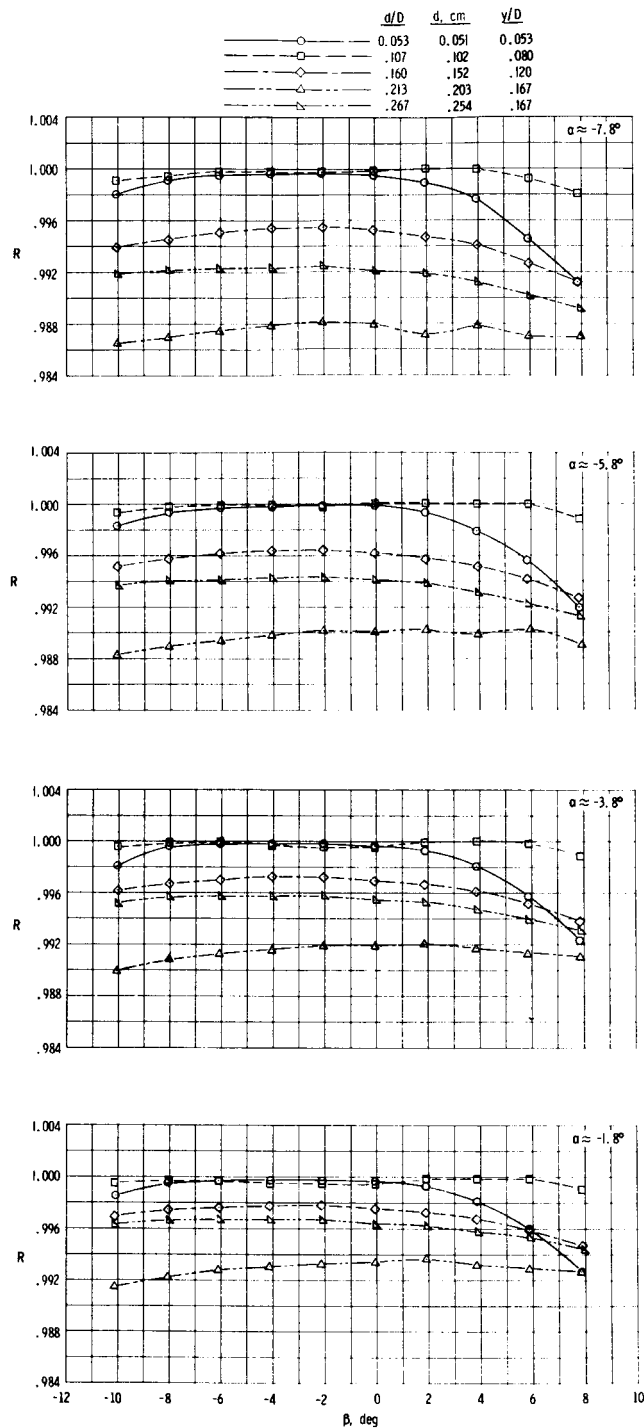
(b) $M = 1.83$.

Figure 5.- Effect of variation of pitot-tube size on the total-pressure recovery throughout the angle-of-attack range. $r/D = 6.0$; $\beta \approx 0^\circ$; $p_{t,1} = 103.42 \text{ kPa}$.



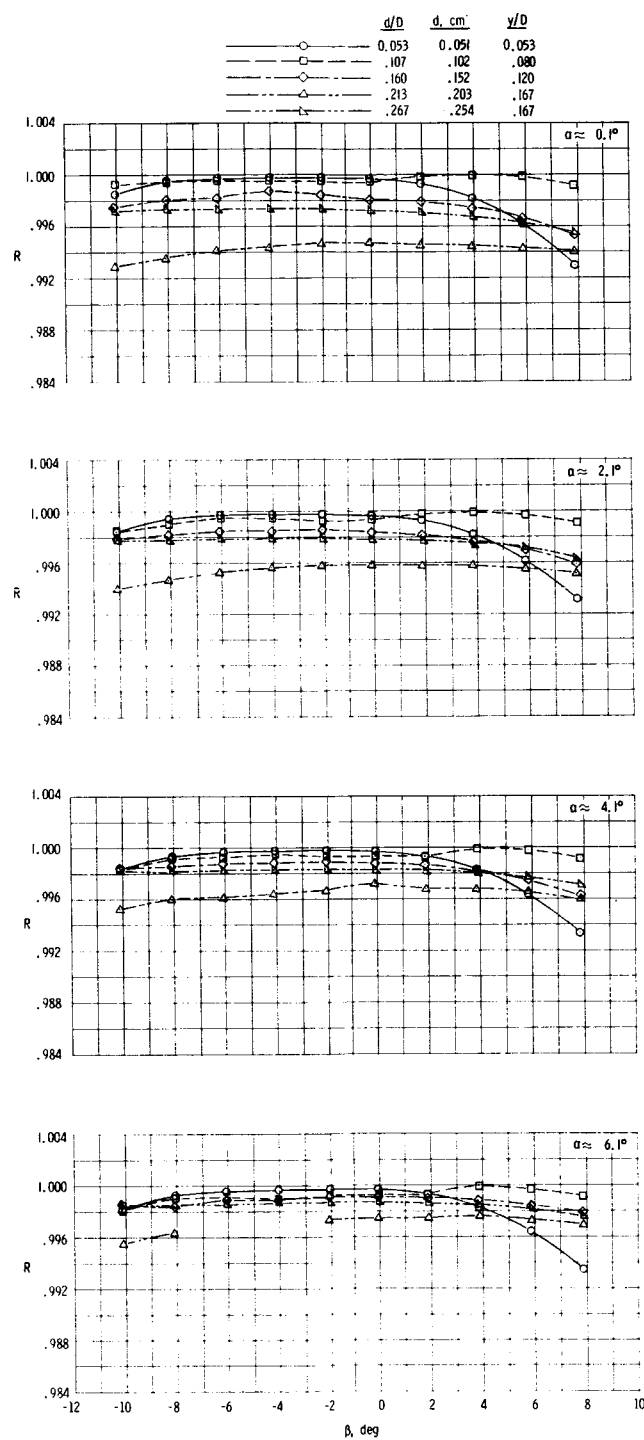
(c) $M = 2.20$.

Figure 5.- Concluded.



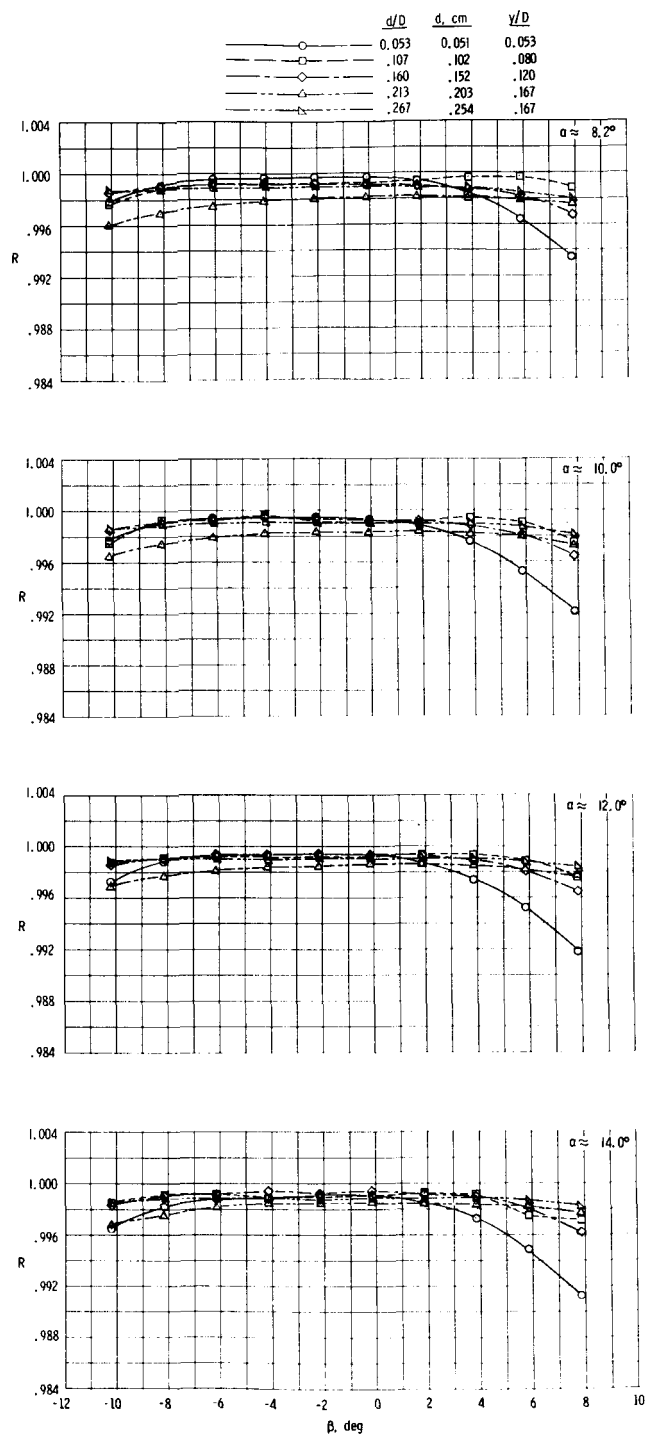
(a) $-7.8^\circ \leq \alpha \leq -1.8^\circ$.

Figure 6.- Effect of variation of pitot-tube size on the total-pressure recovery throughout the angle-of-yaw range at discrete angles of attack and a Mach number of 1.41. $r/D = 6.0$; $p_{t,1} = 103.42 \text{ kPa}$.



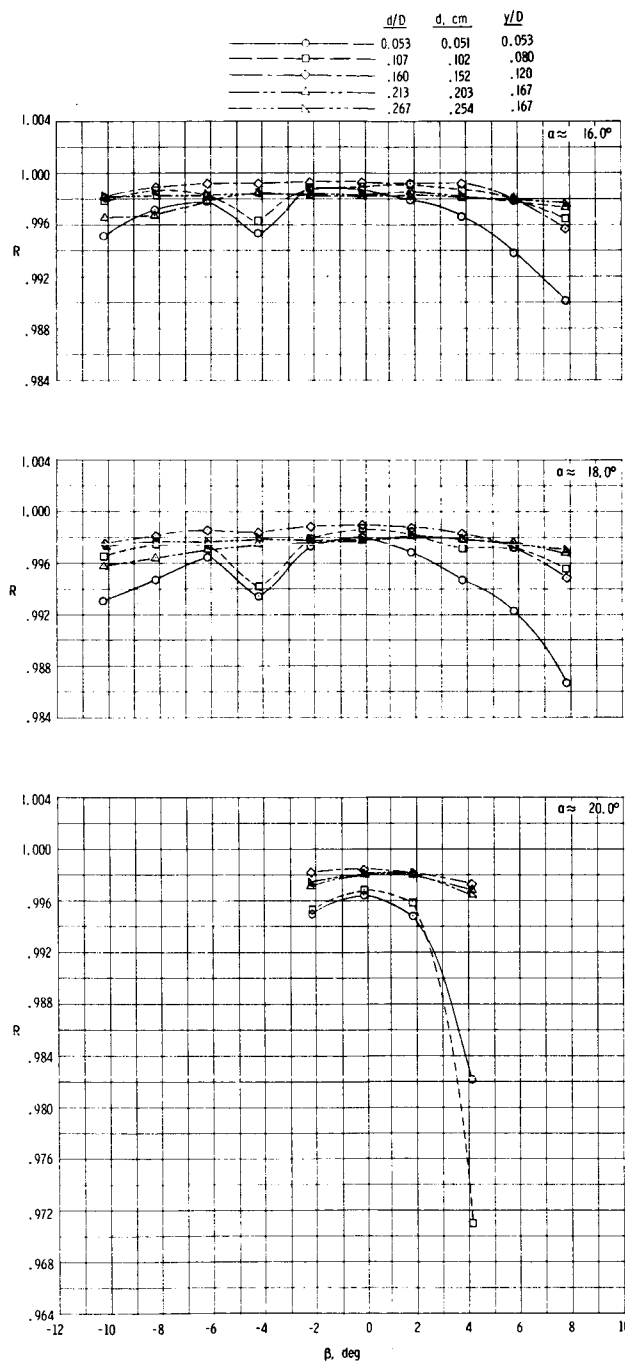
(b) $0.1^\circ \leq \alpha \leq 6.1^\circ$.

Figure 6.- Continued.



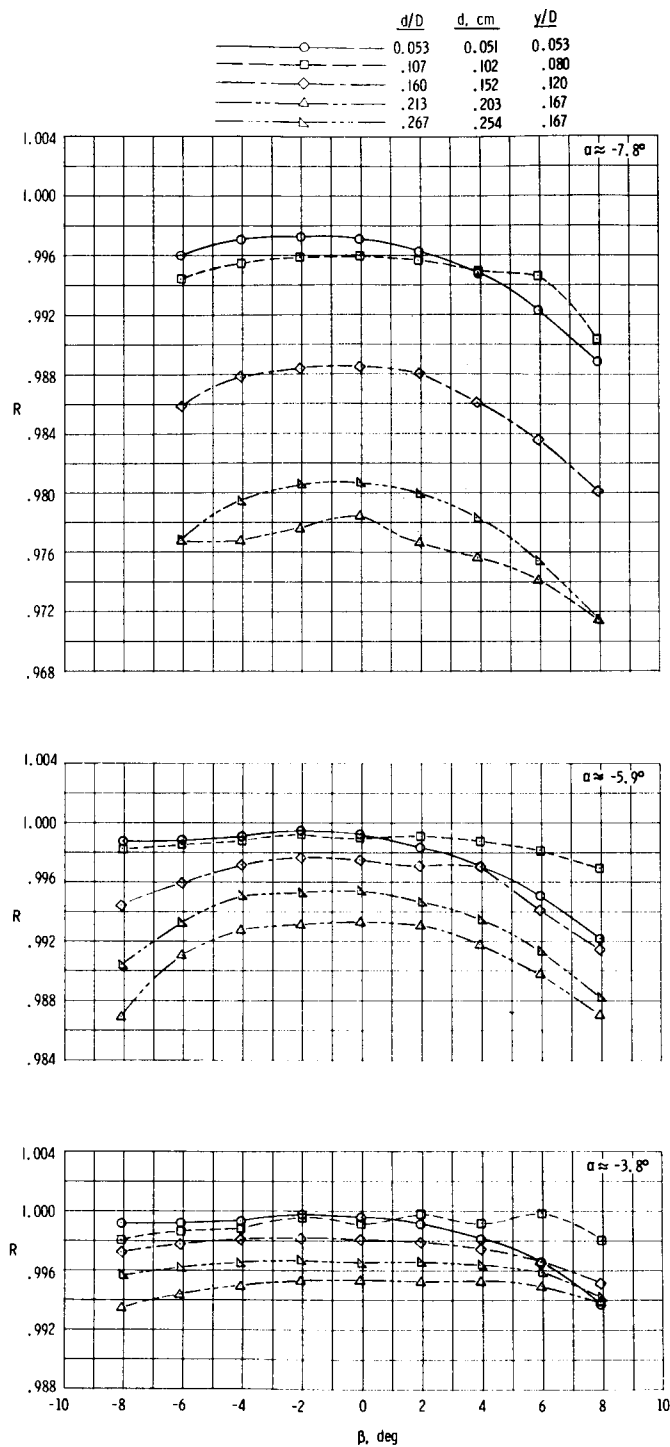
(c) $8.2^\circ \leq \alpha \leq 14.0^\circ$.

Figure 6.- Continued.



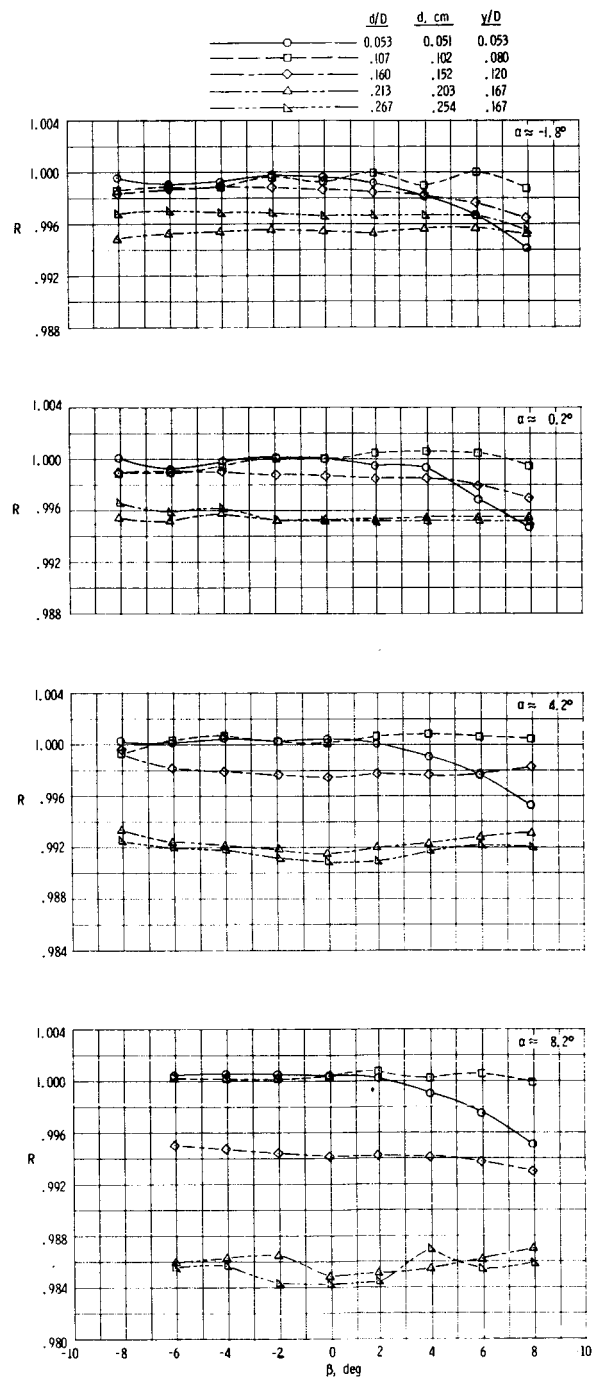
(d) $16.0^\circ \leq \alpha \leq 20.0^\circ$.

Figure 6.- Concluded.



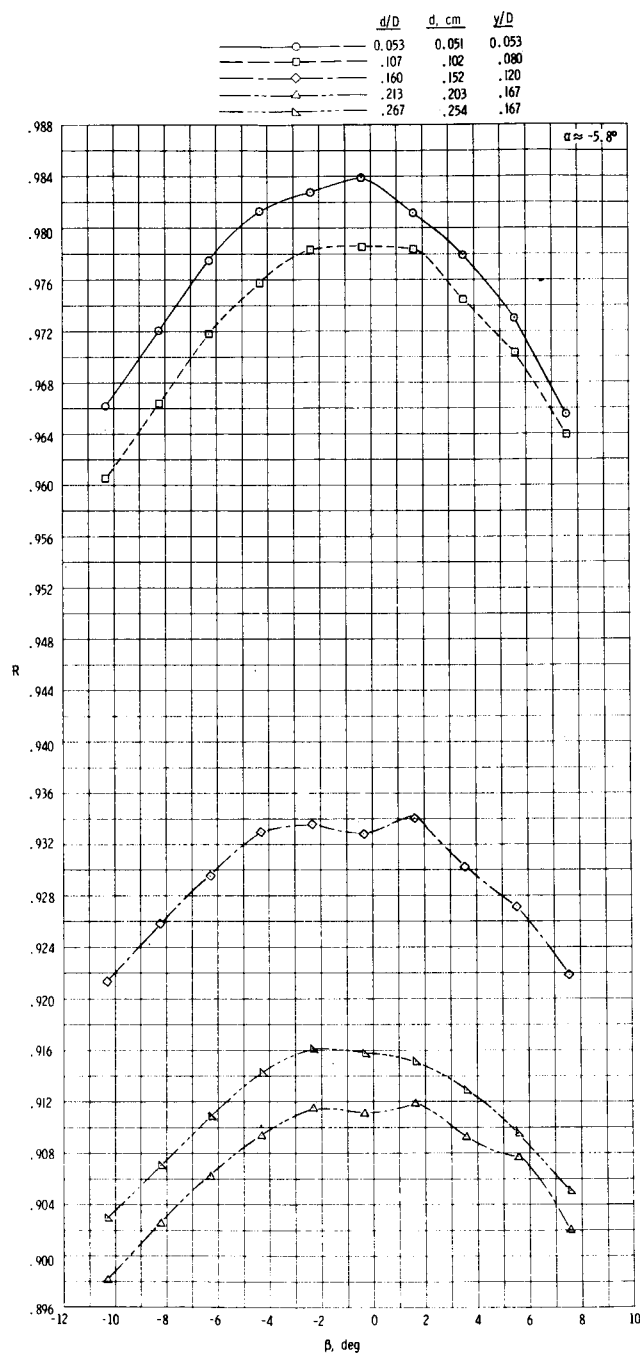
(a) $-7.8^\circ \leq \alpha \leq -3.8^\circ$.

Figure 7.- Effect of variation of pitot-tube size on the total-pressure recovery throughout the angle-of-yaw range at discrete angles of attack and a Mach number of 1.83. $r/D = 6.0$; $p_{t,1} = 103.42 \text{ kPa}$.



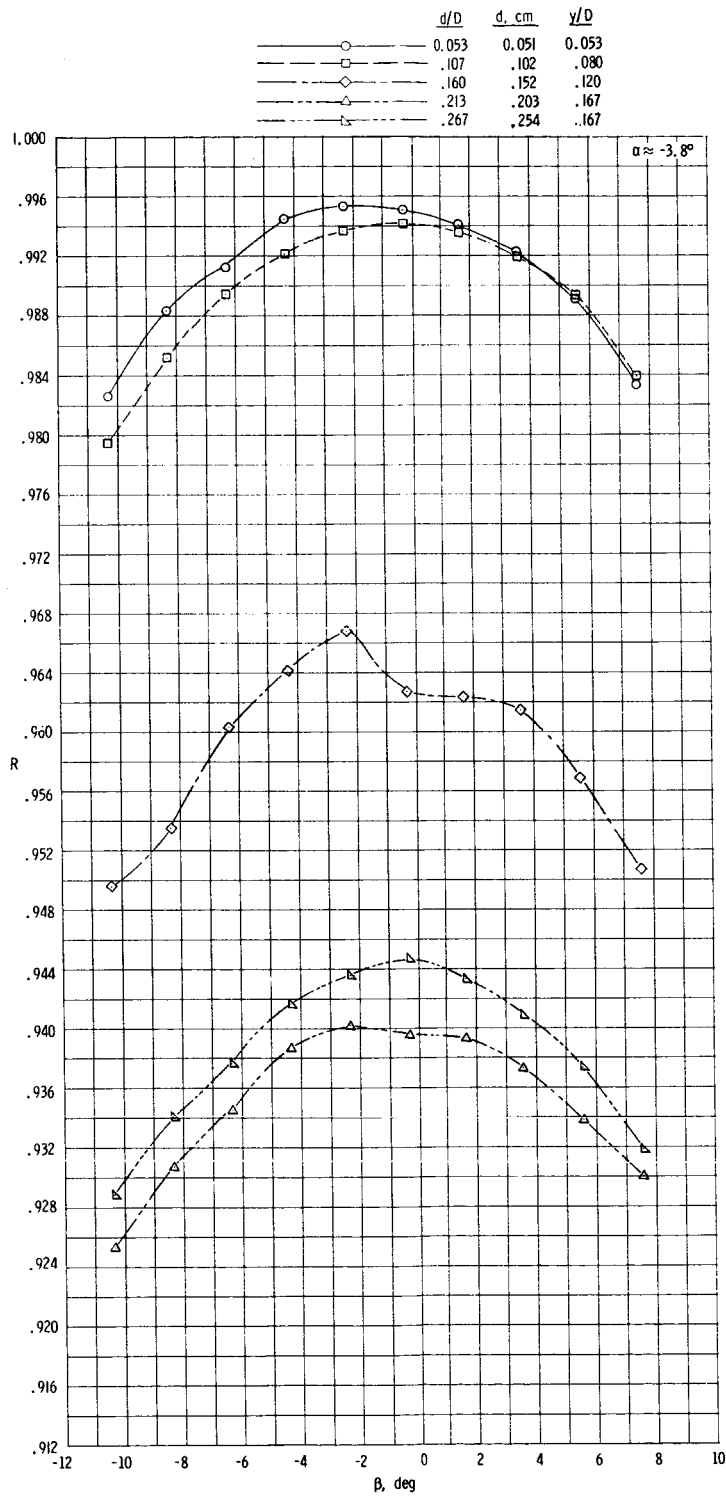
(b) $-1.8^\circ \leq \alpha \leq 8.2^\circ$.

Figure 7.- Concluded.



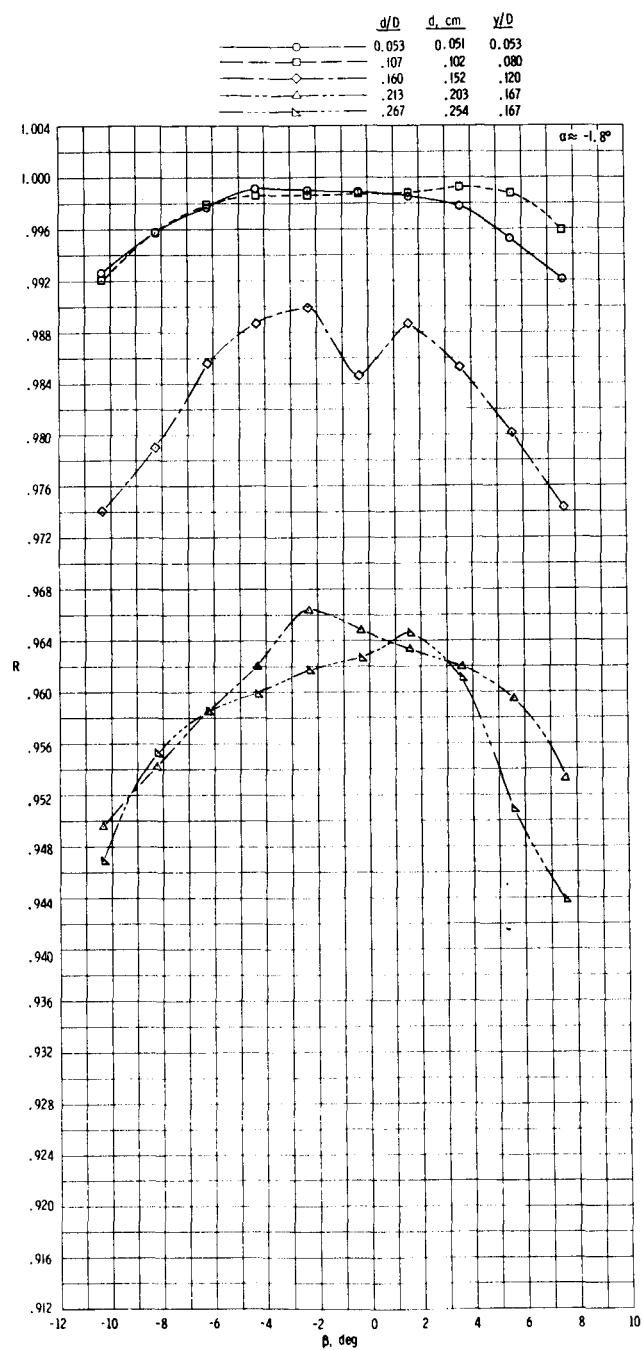
(a) $\alpha \approx -5.8^\circ$.

Figure 8.- Effect of variation of pitot-tube size on the total-pressure recovery throughout the angle-of-yaw range at discrete angles of attack and a Mach number of 2.20. $r/D = 6.0$; $p_{t,1} = 103.42 \text{ kPa}$.



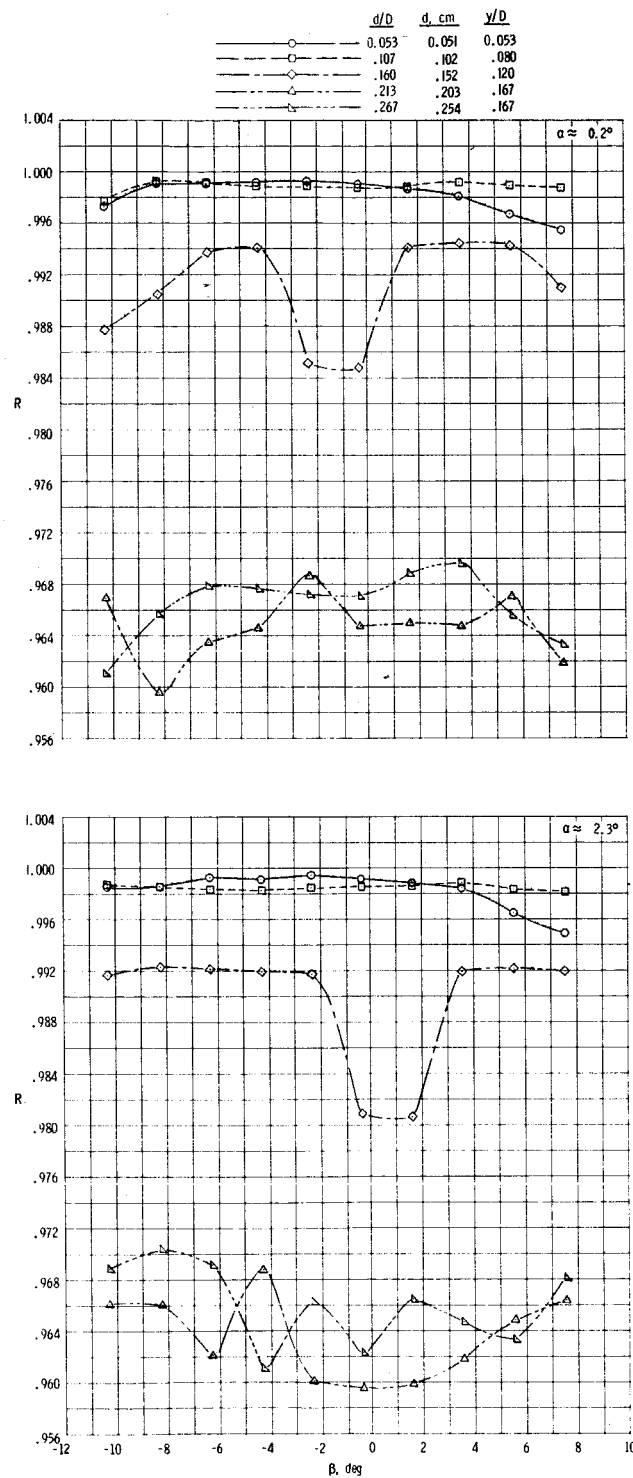
(b) $\alpha \approx -3.8^\circ$.

Figure 8.- Continued.



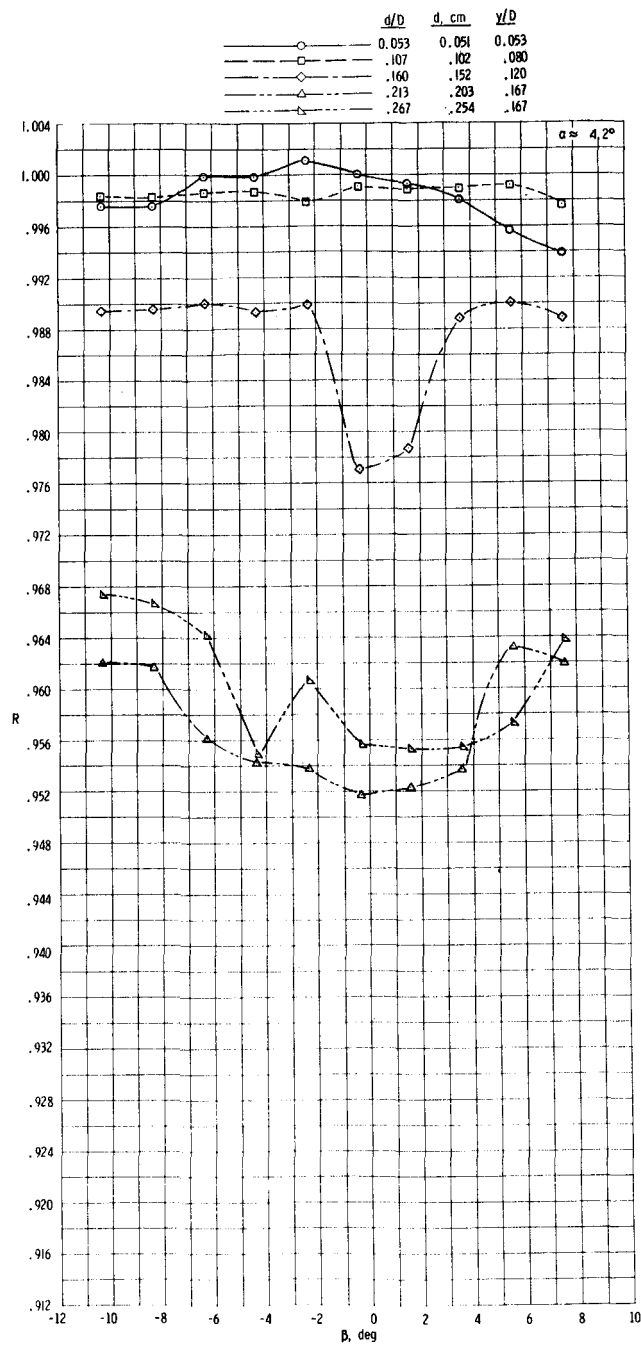
(c) $\alpha \approx -1.8^\circ$.

Figure 8.- Continued.



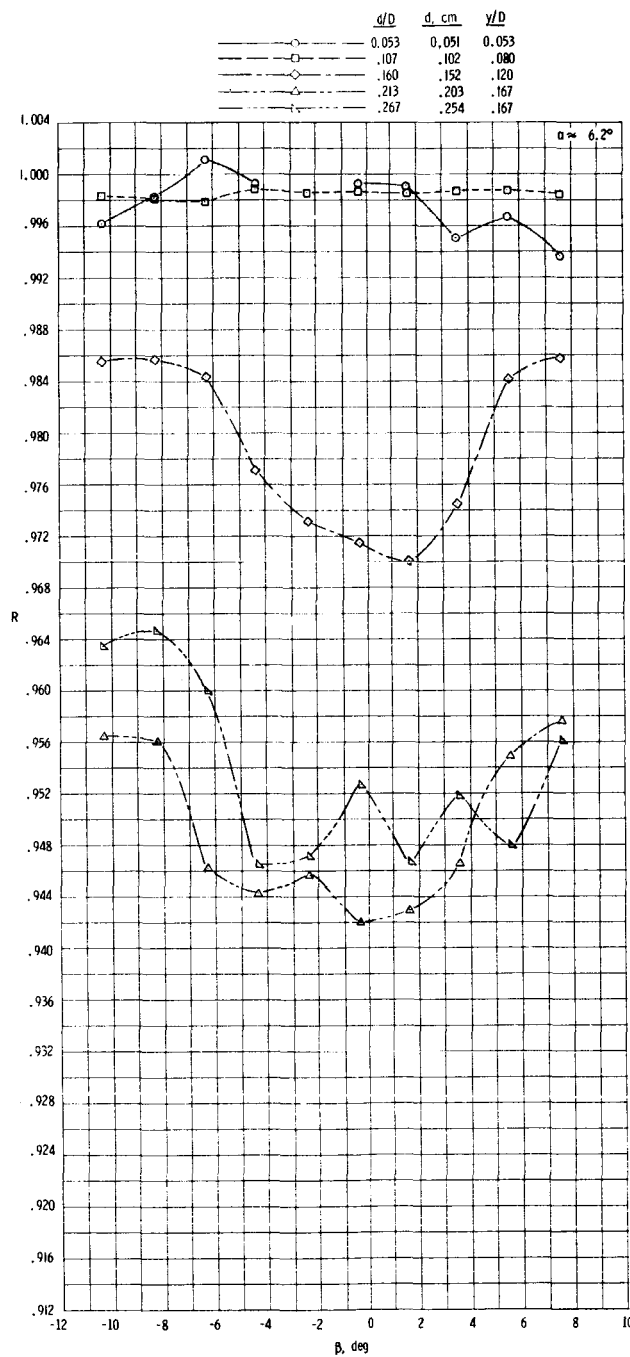
(d) $0.2^\circ \leq \alpha \leq 2.3^\circ$.

Figure 8.- Continued.



(e) $\alpha \approx 4.2^\circ$.

Figure 8.- Continued.



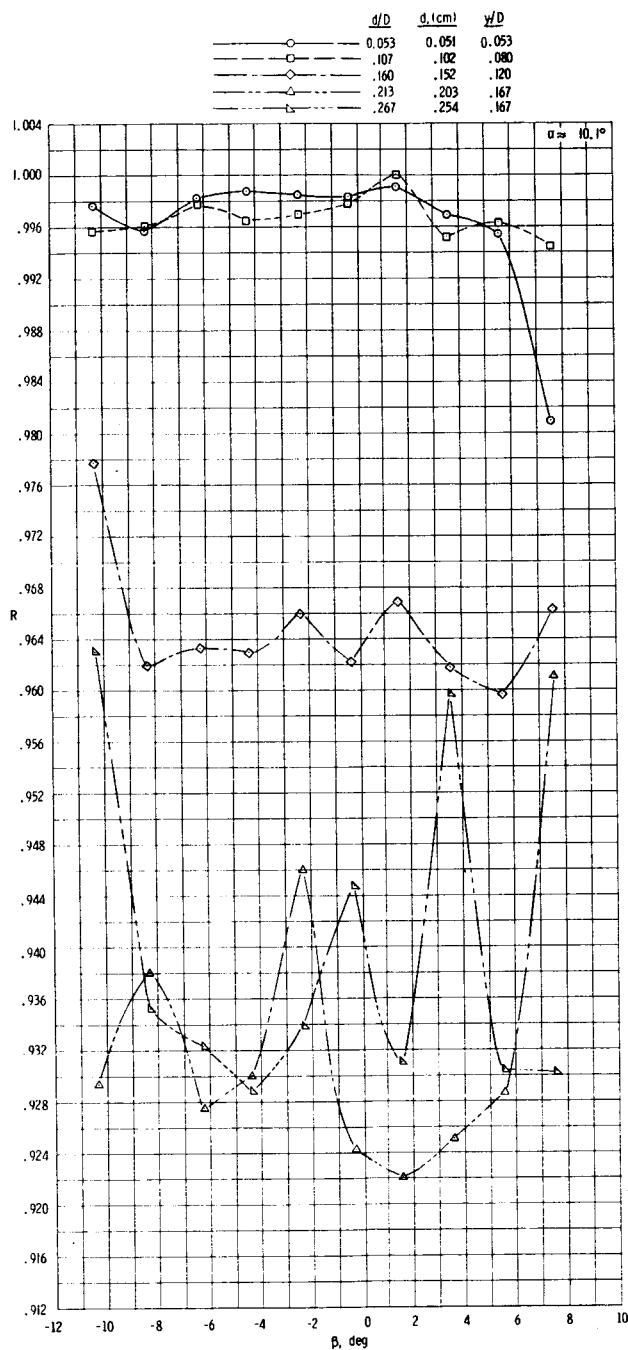
(f) $\alpha \approx 6.2^\circ$.

Figure 8.- Continued.



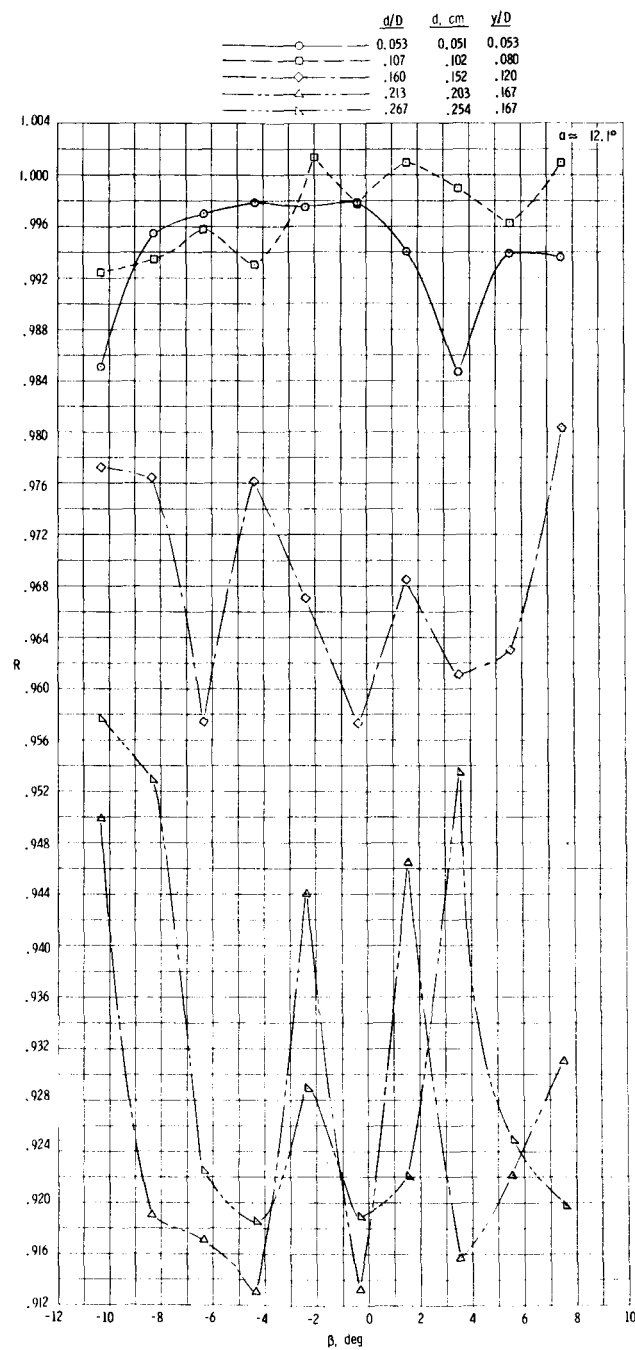
(g) $\alpha \approx 8.2^\circ$.

Figure 8.- Continued.



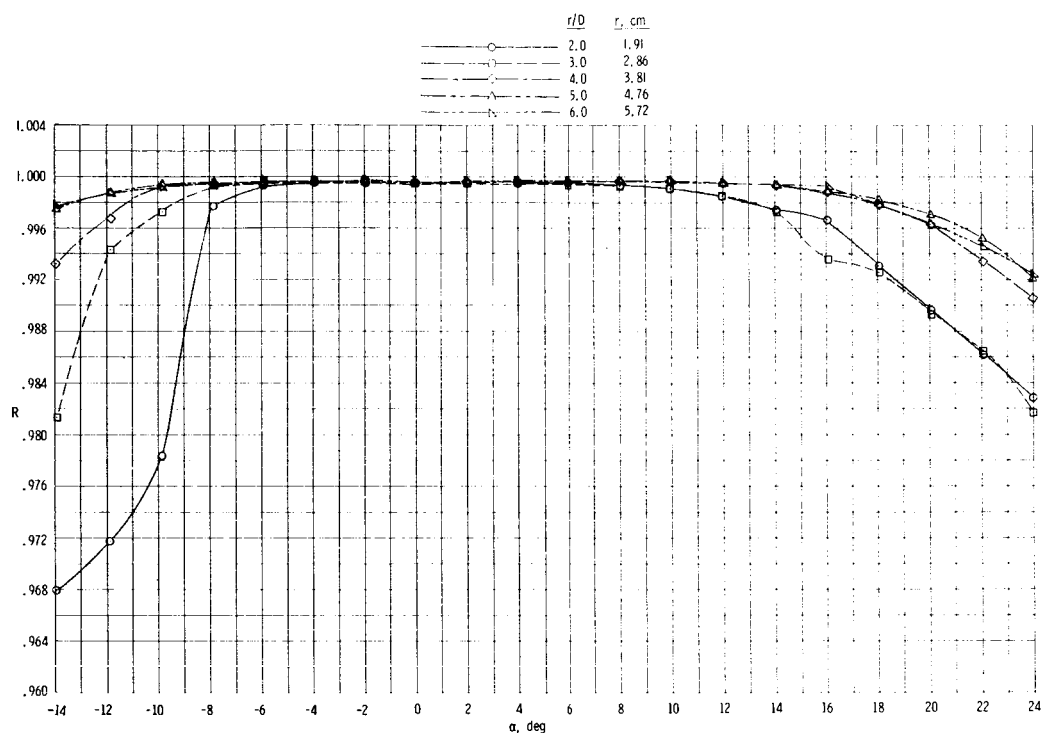
(h) $\alpha \approx 10.1^\circ$.

Figure 8.- Continued.

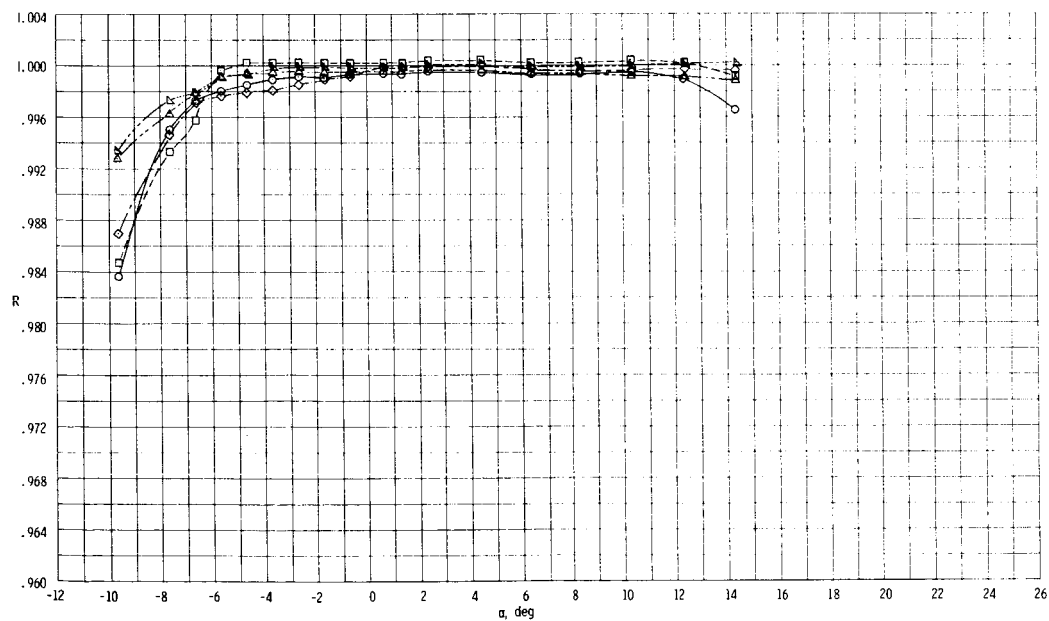


(i) $\alpha \approx 12.1^\circ$.

Figure 8.- Concluded.

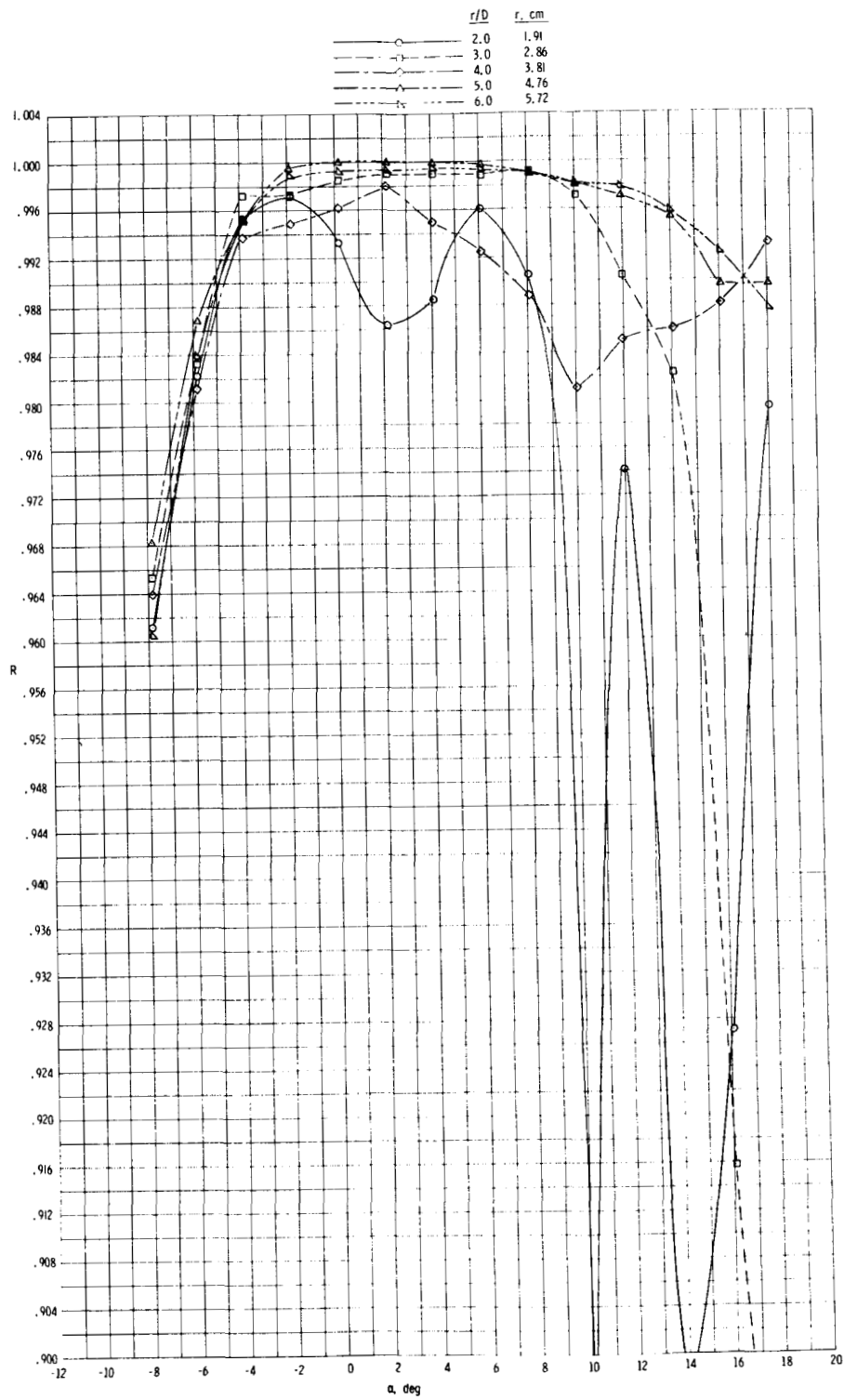


(a) $M = 1.41$.



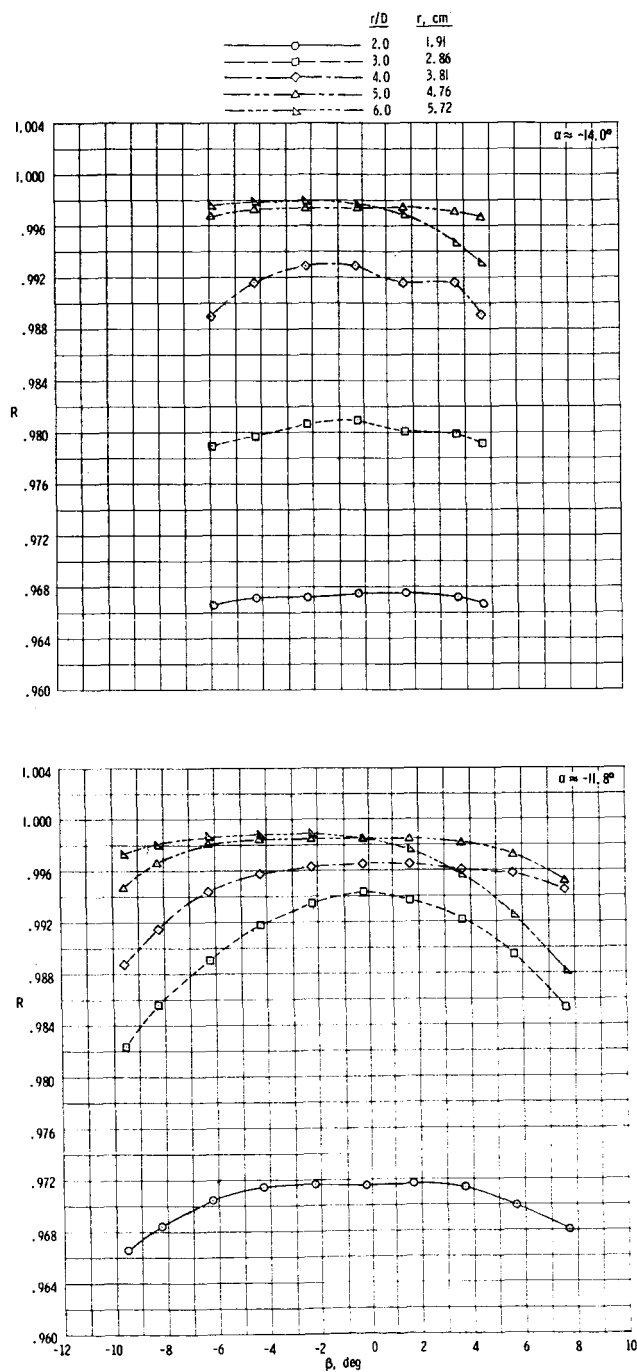
(b) $M = 1.83$.

Figure 9.- Effect of variation of surface curvature on the total-pressure recovery throughout the angle-of-attack range. $y/D = 0.053$; $\beta \approx 0^\circ$; $p_{t,1} = 103.42 \text{ kPa}$.



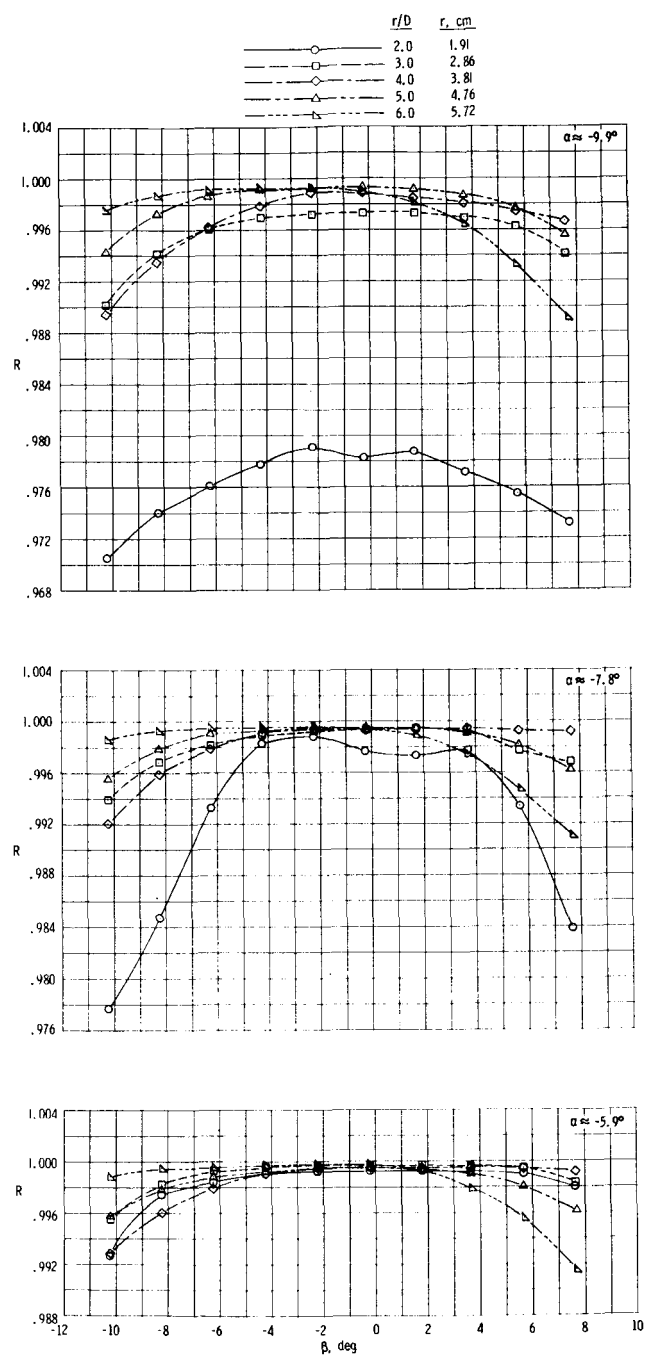
(c) $M = 2.20$.

Figure 9.- Concluded.



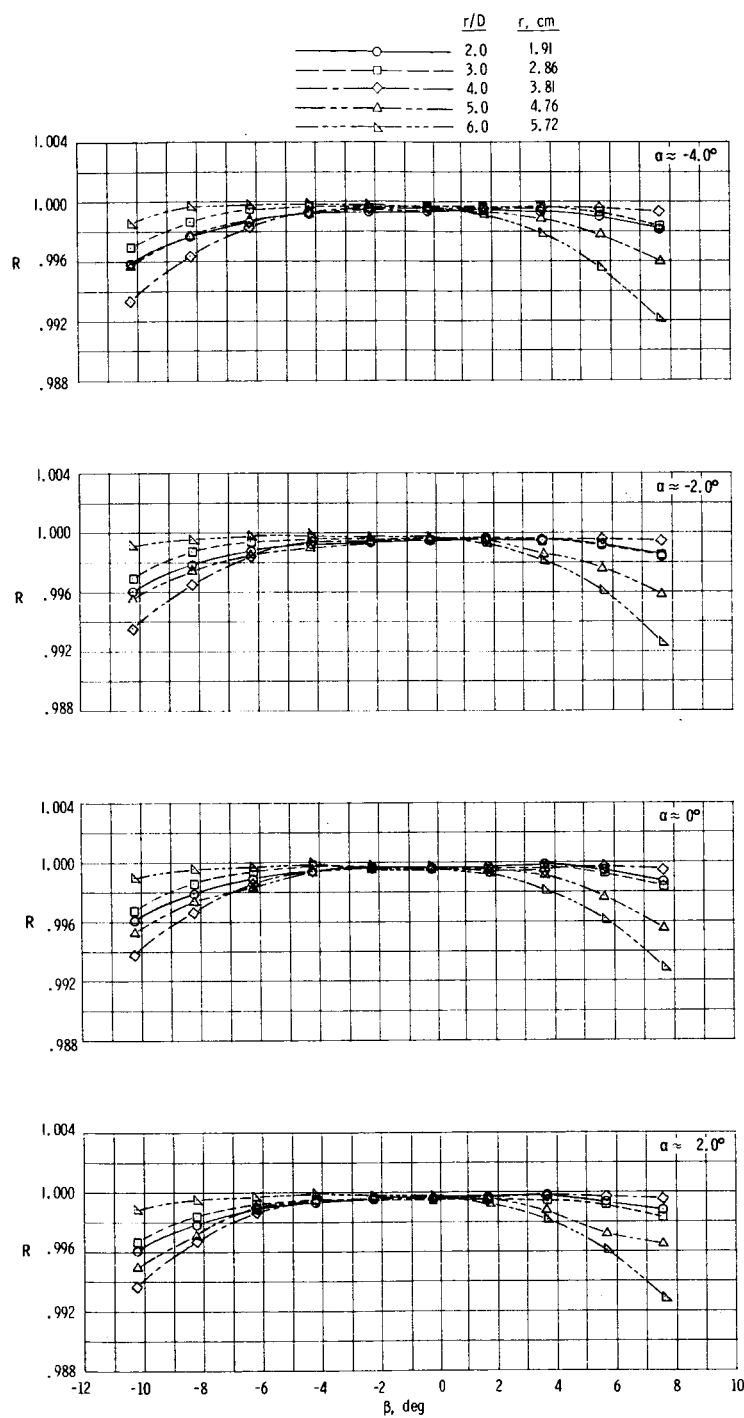
(a) $-14.0^\circ \leq \alpha \leq -11.8^\circ$.

Figure 10.- Effect of variation of surface curvature on the total-pressure recovery throughout the angle-of-yaw range at discrete angles of attack and a Mach number of 1.41. $y/D = 0.053$; $p_{t,1} = 103.42 \text{ kPa}$.



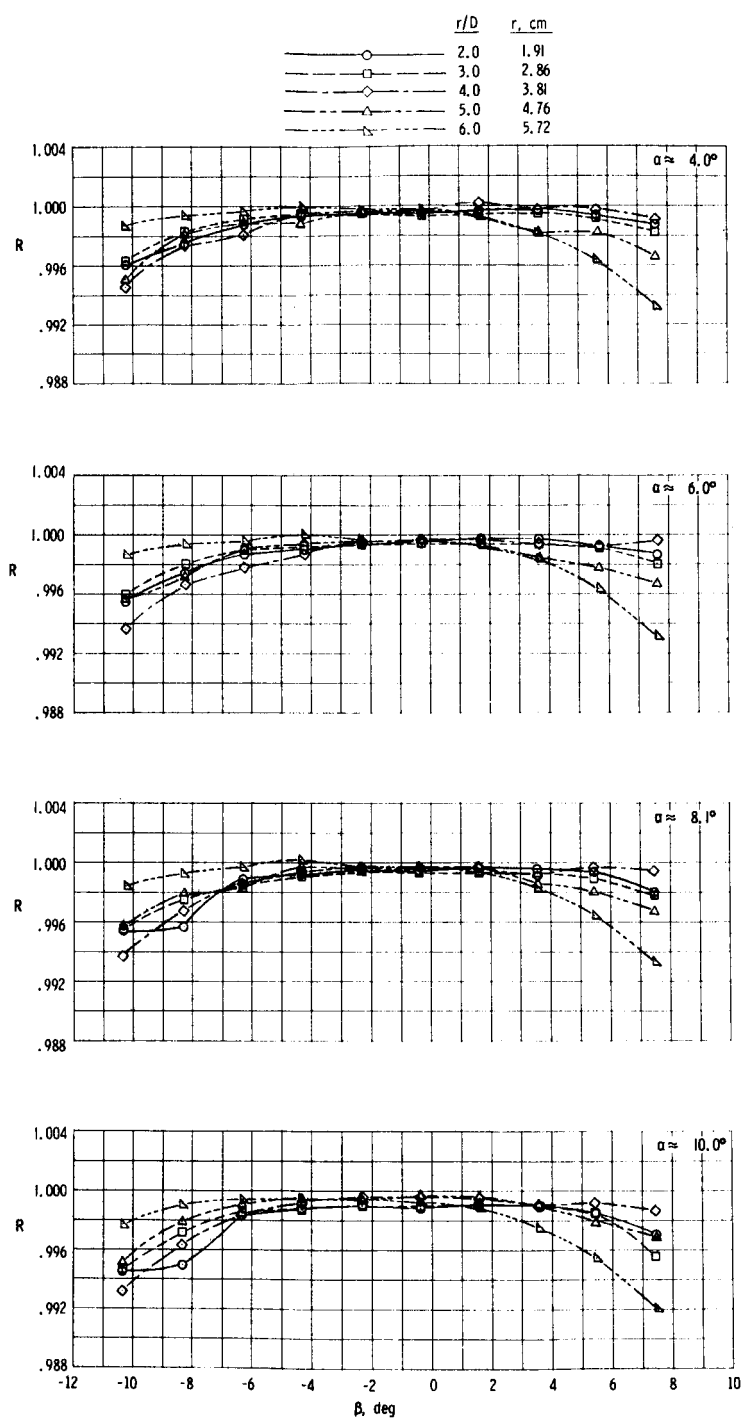
(b) $-9.9^\circ \leq \alpha \leq -5.9^\circ$.

Figure 10.- Continued.



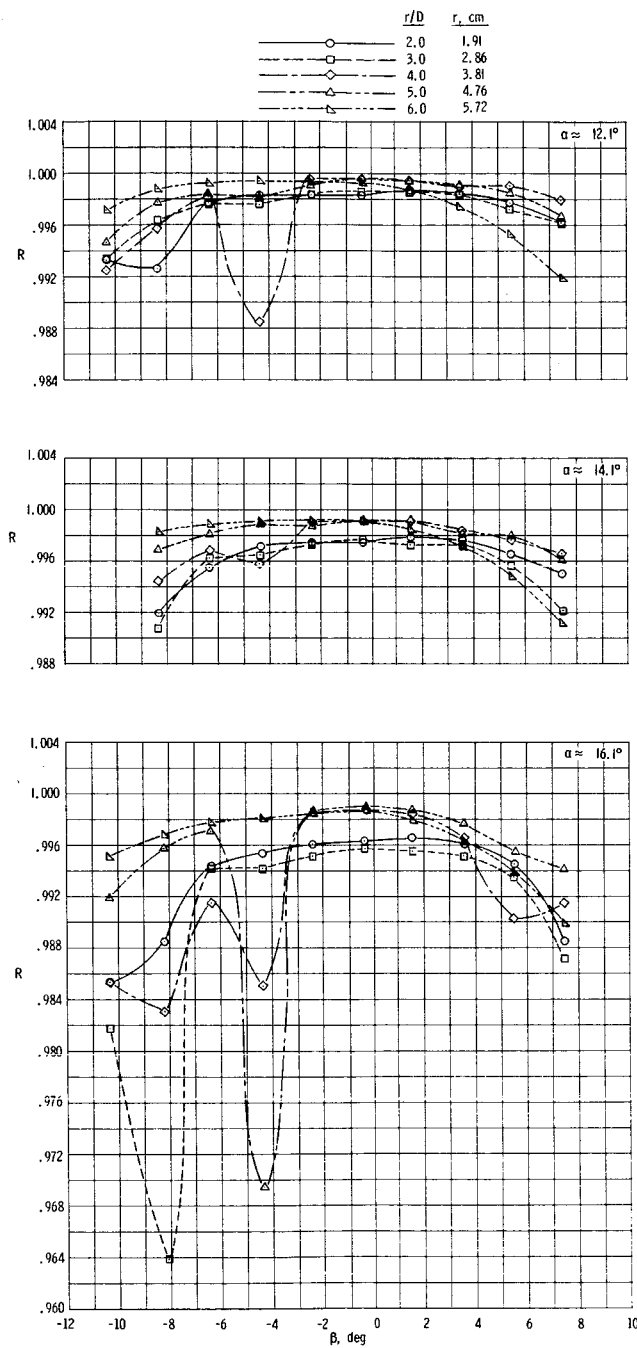
(c) $-4.0^\circ \leq \alpha \leq 2.0^\circ$.

Figure 10.- Continued.



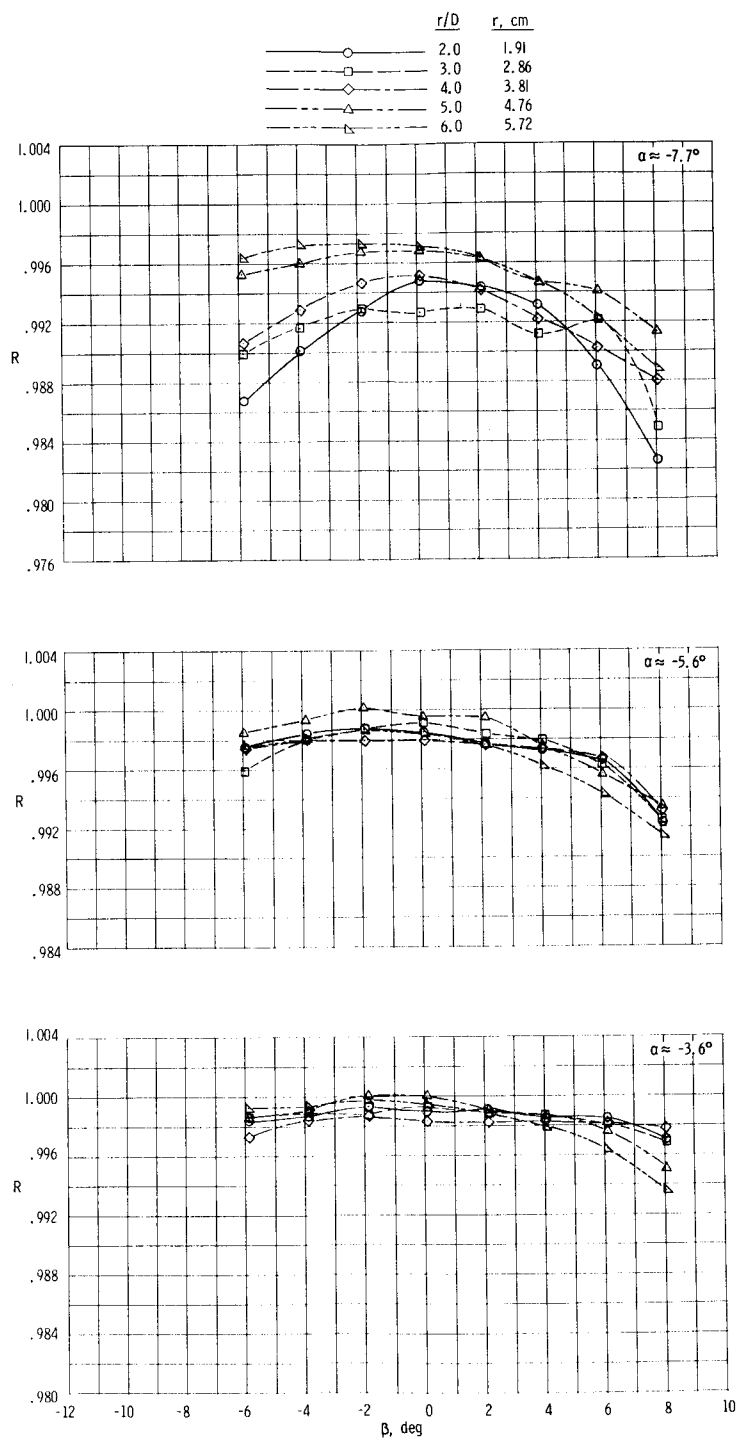
(d) $4.0^\circ \leq \alpha \leq 10.0^\circ$.

Figure 10.- Continued.



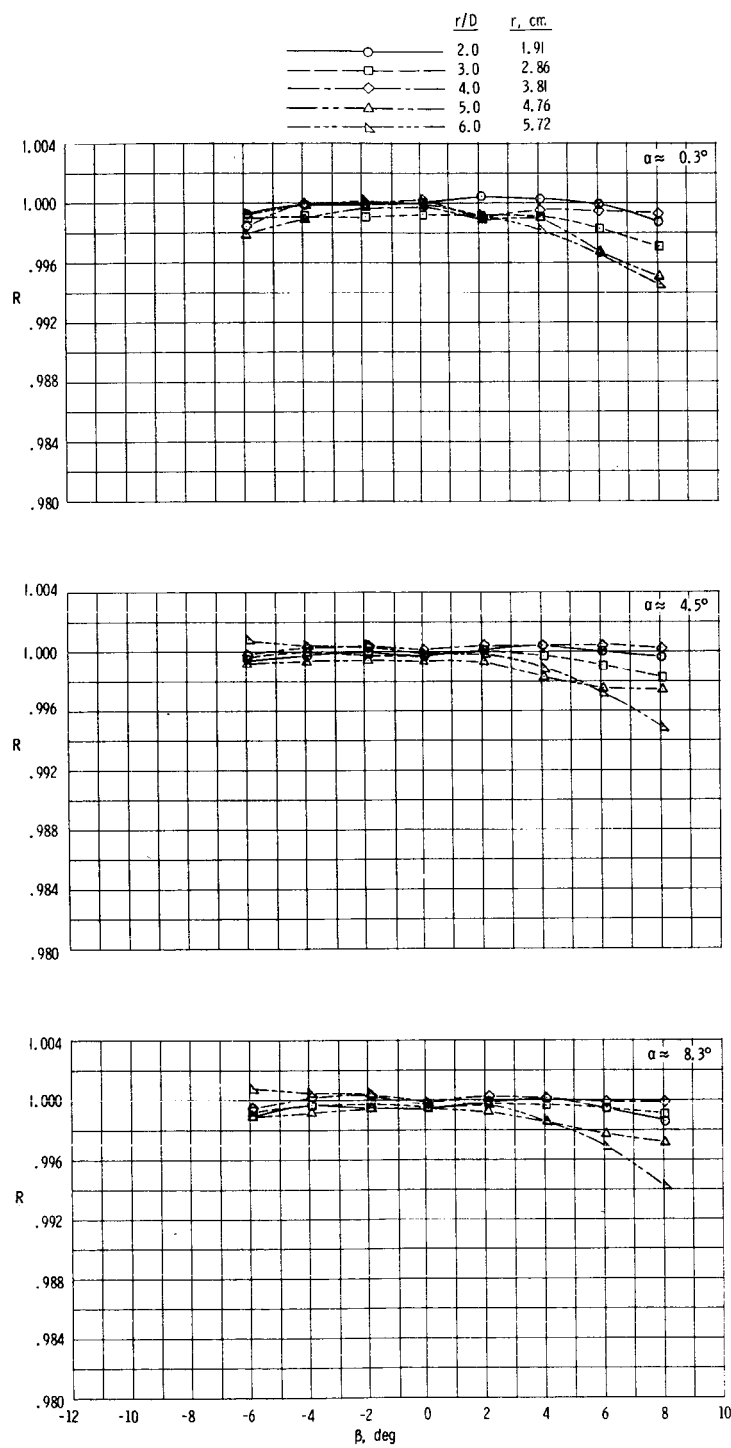
(e) $12.1^\circ \leq \alpha \leq 16.1^\circ$.

Figure 10.- Concluded.



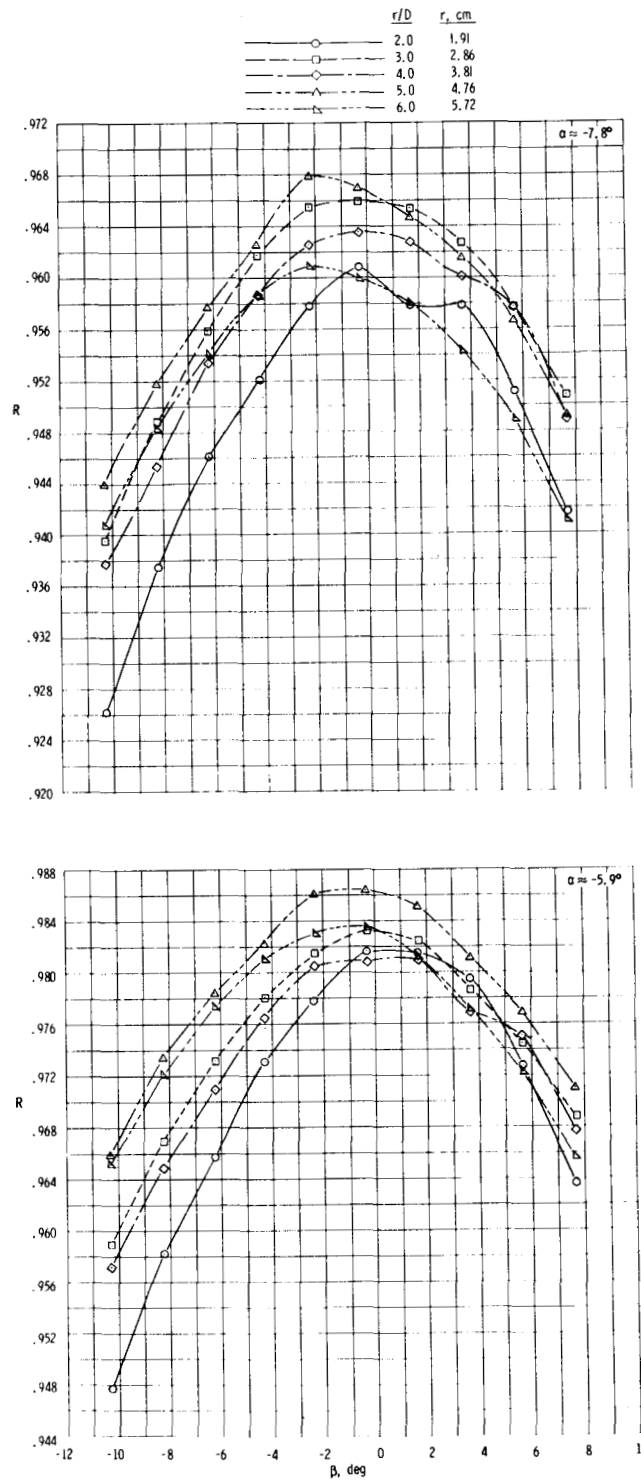
(a) $-7.7^\circ \leq \alpha \leq -3.6^\circ$.

Figure 11.- Effect of variation of surface curvature on the total-pressure recovery throughout the angle-of-yaw range at discrete angles of attack and a Mach number of 1.83. $y/D = 0.053$; $p_{t,1} = 103.42 \text{ kPa}$.



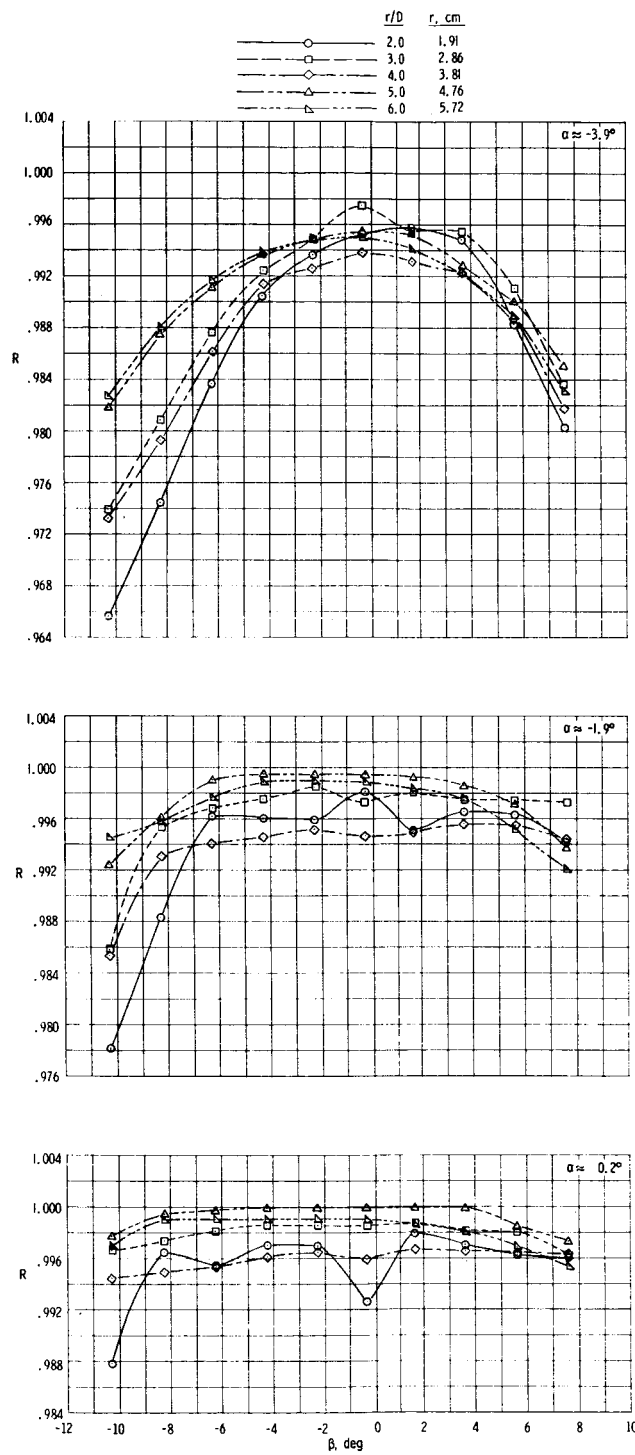
(b) $0.3^\circ \leq \alpha \leq 8.3^\circ$.

Figure 11.- Concluded.



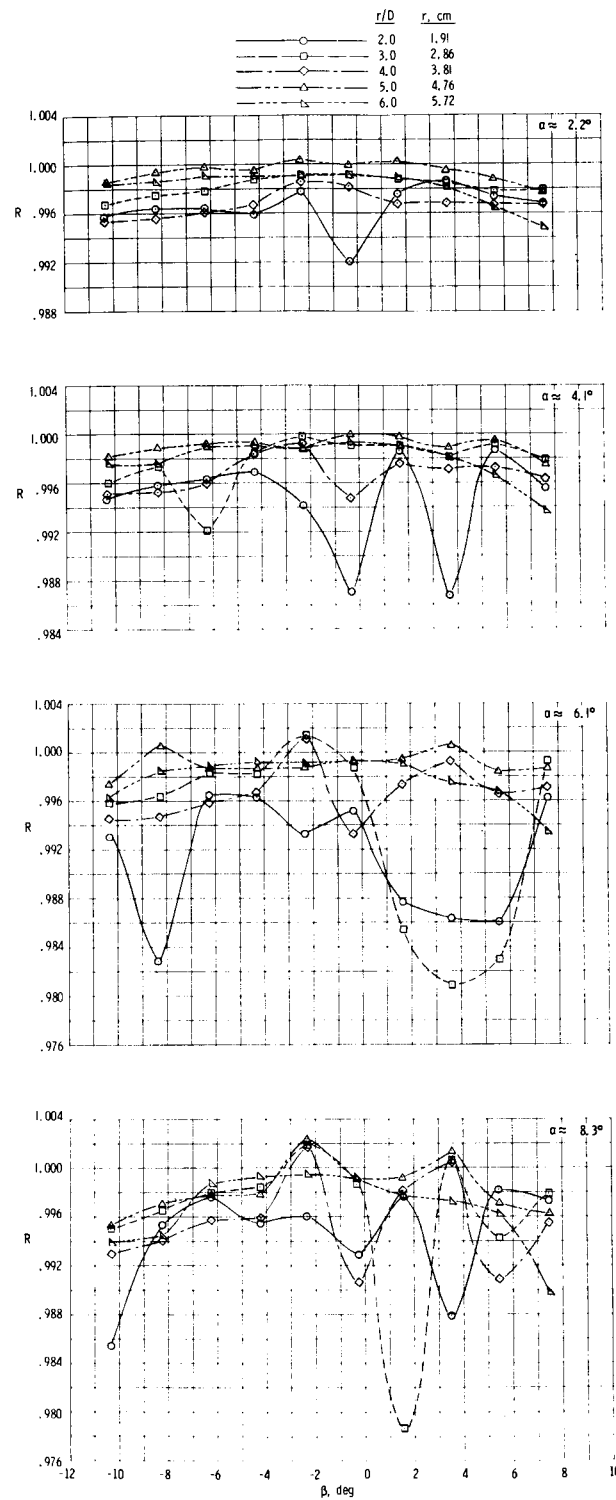
(a) $-7.8^\circ \leq \alpha \leq -5.9^\circ$.

Figure 12.- Effect of variation of surface curvature on the total-pressure recovery throughout the angle-of-yaw range at discrete angles of attack and a Mach number of 2.20. $y/D = 0.053$; $p_{t,1} = 103.42 \text{ kPa}$.



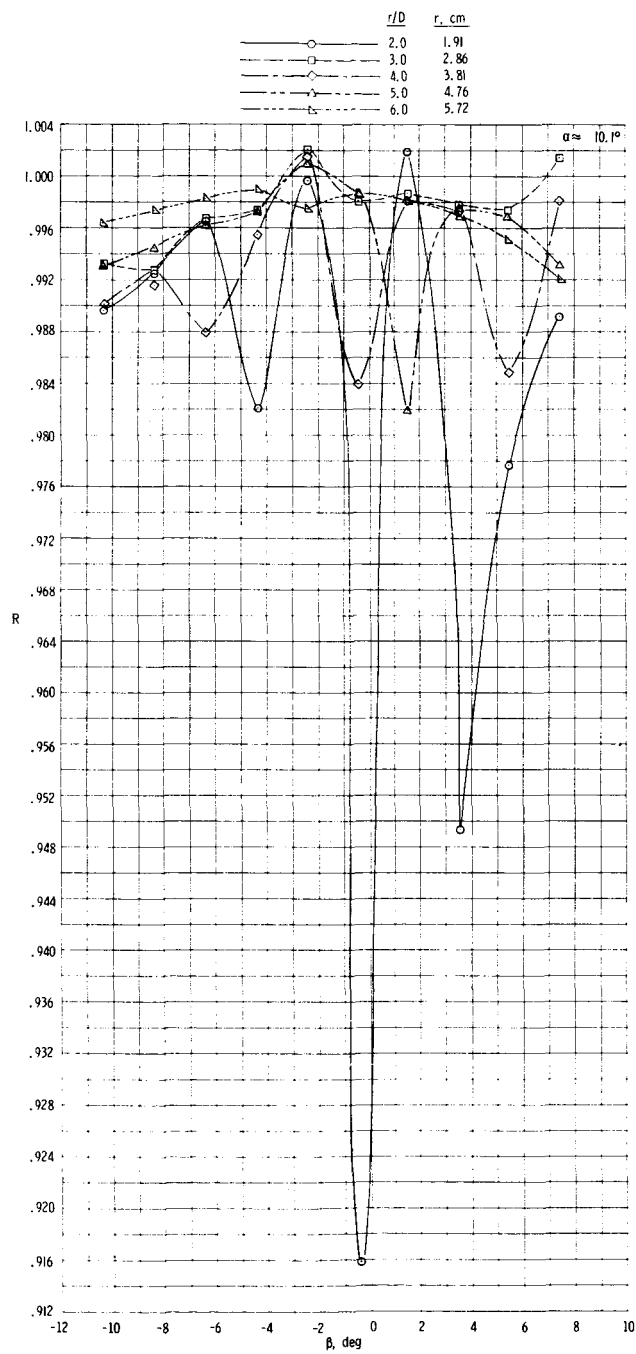
(b) $-3.9^\circ \leq \alpha \leq 0.2^\circ$.

Figure 12.- Continued.



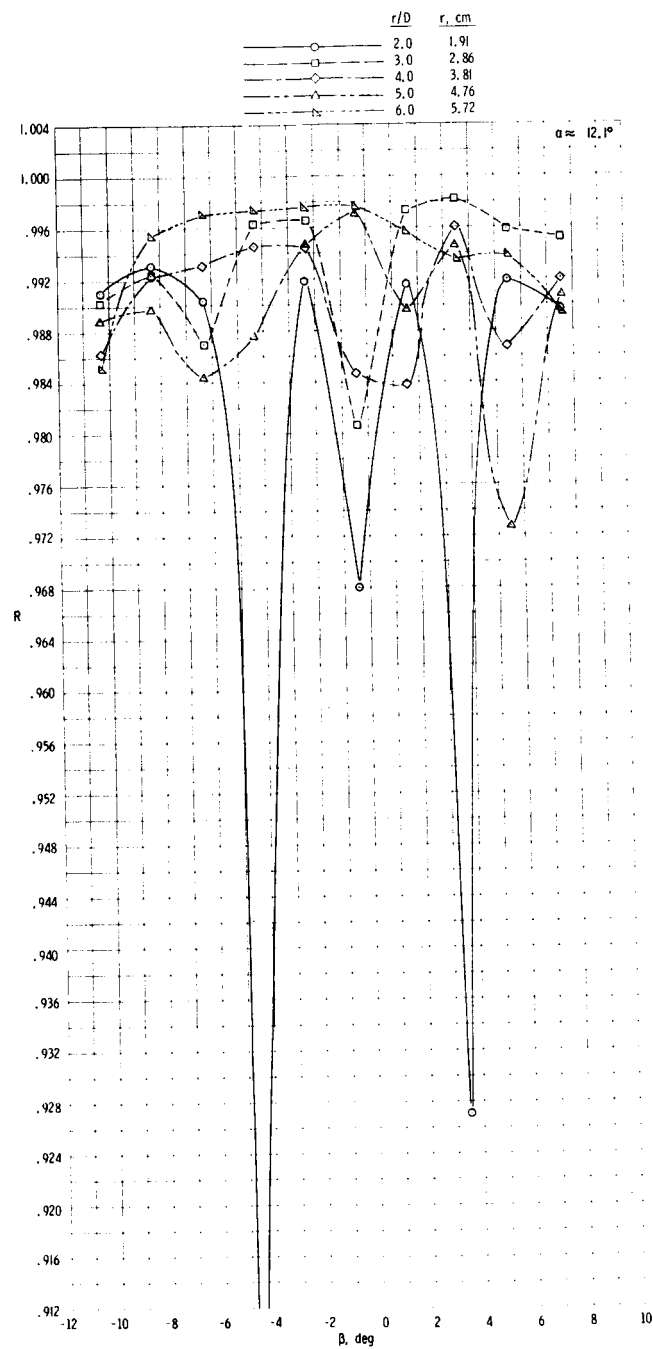
(c) $2.2^\circ \leq \alpha \leq 8.3^\circ$.

Figure 12.- Continued.



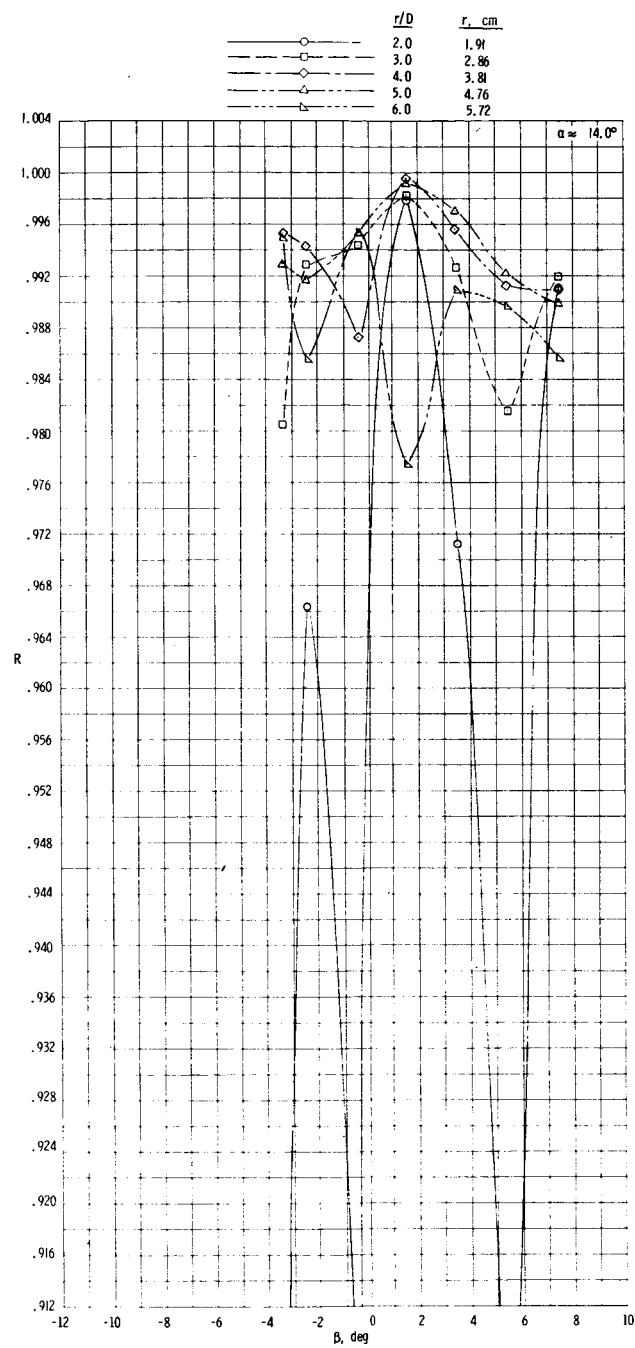
(d) $\alpha \approx 10.1^\circ$.

Figure 12.- Continued.



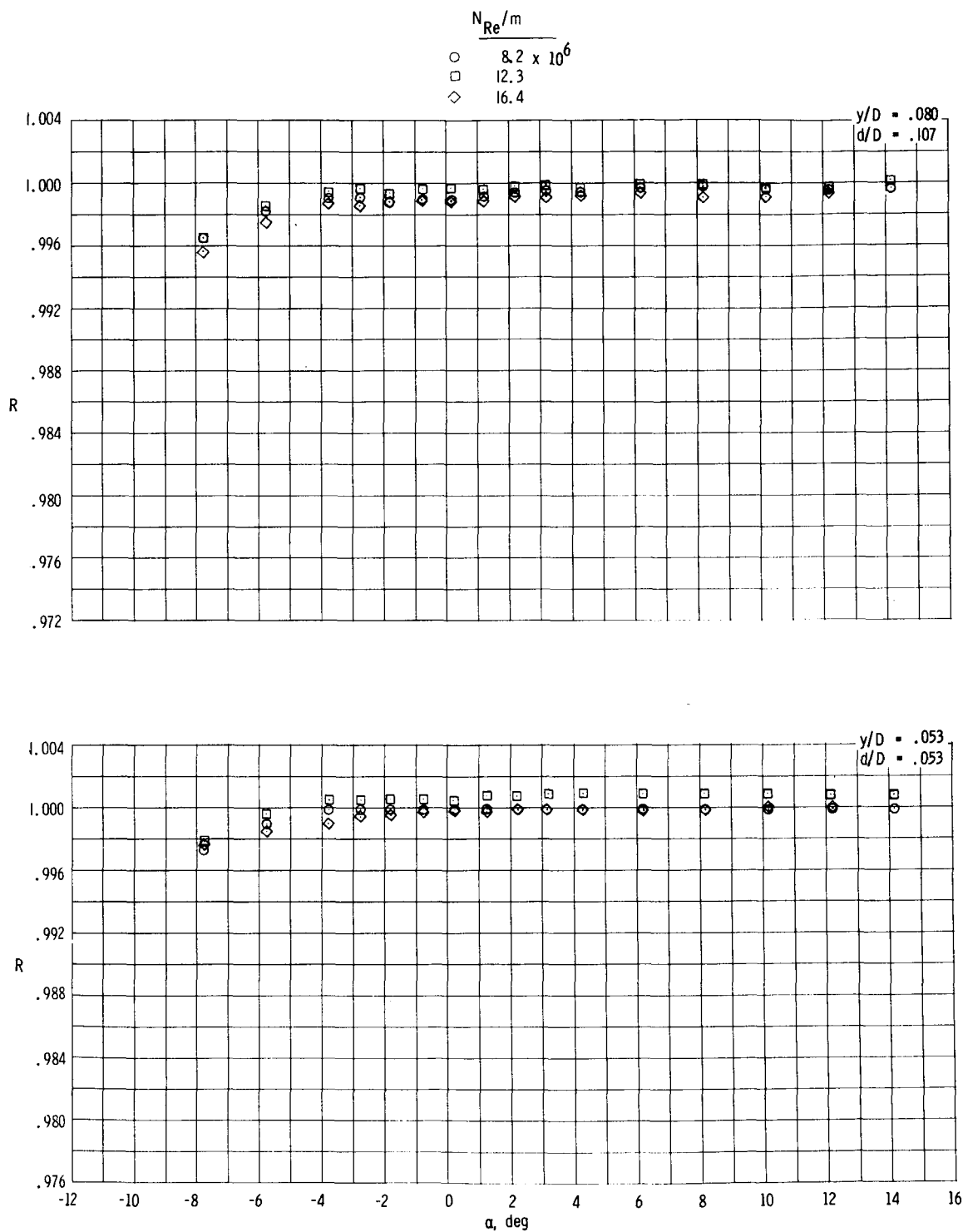
(e) $\alpha \approx 12.1^\circ$.

Figure 12.- Continued.



(f) $\alpha \approx 14.0^\circ$.

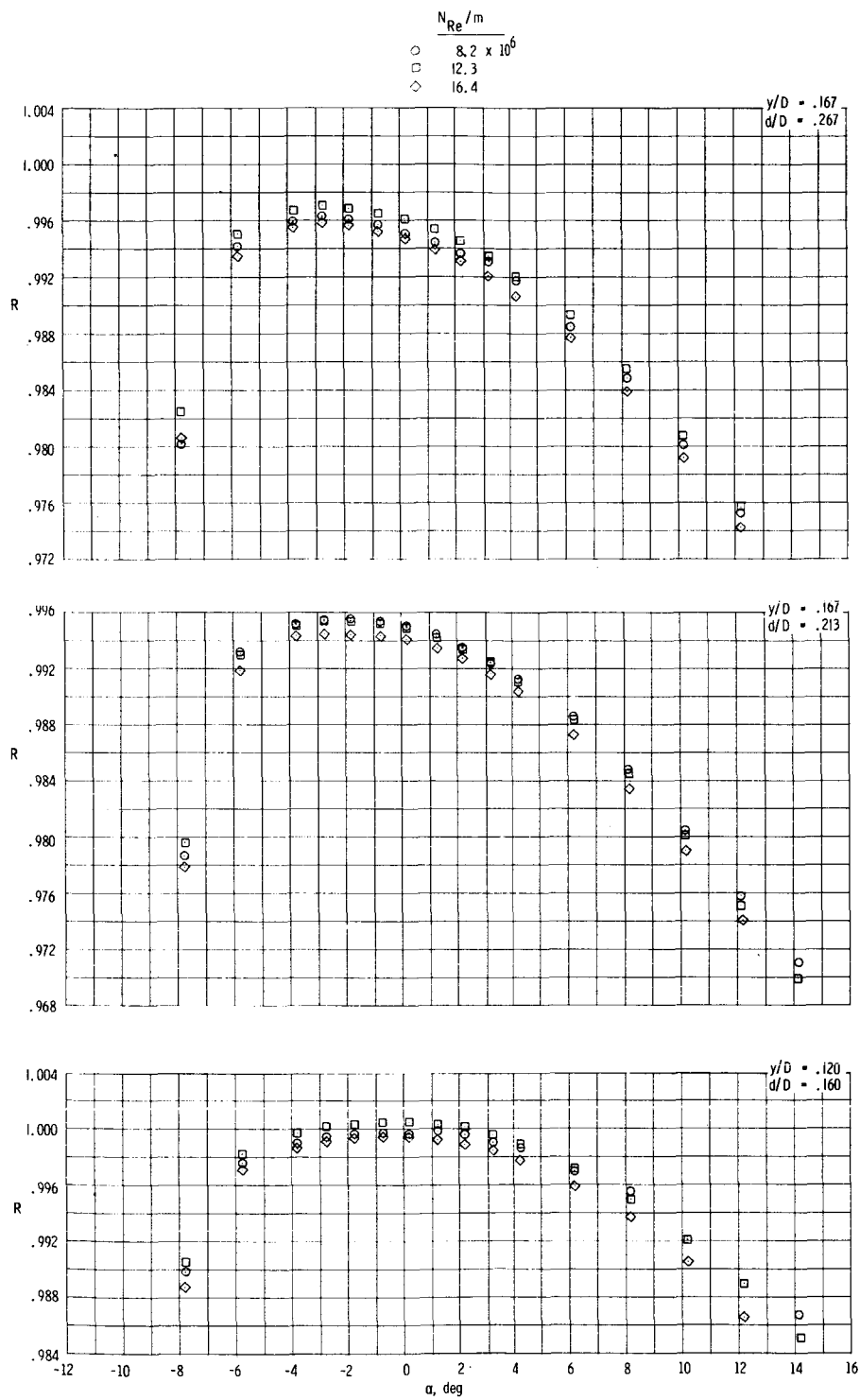
Figure 12.- Concluded.



(a) $0.053 \leq y/D \leq 0.080$.

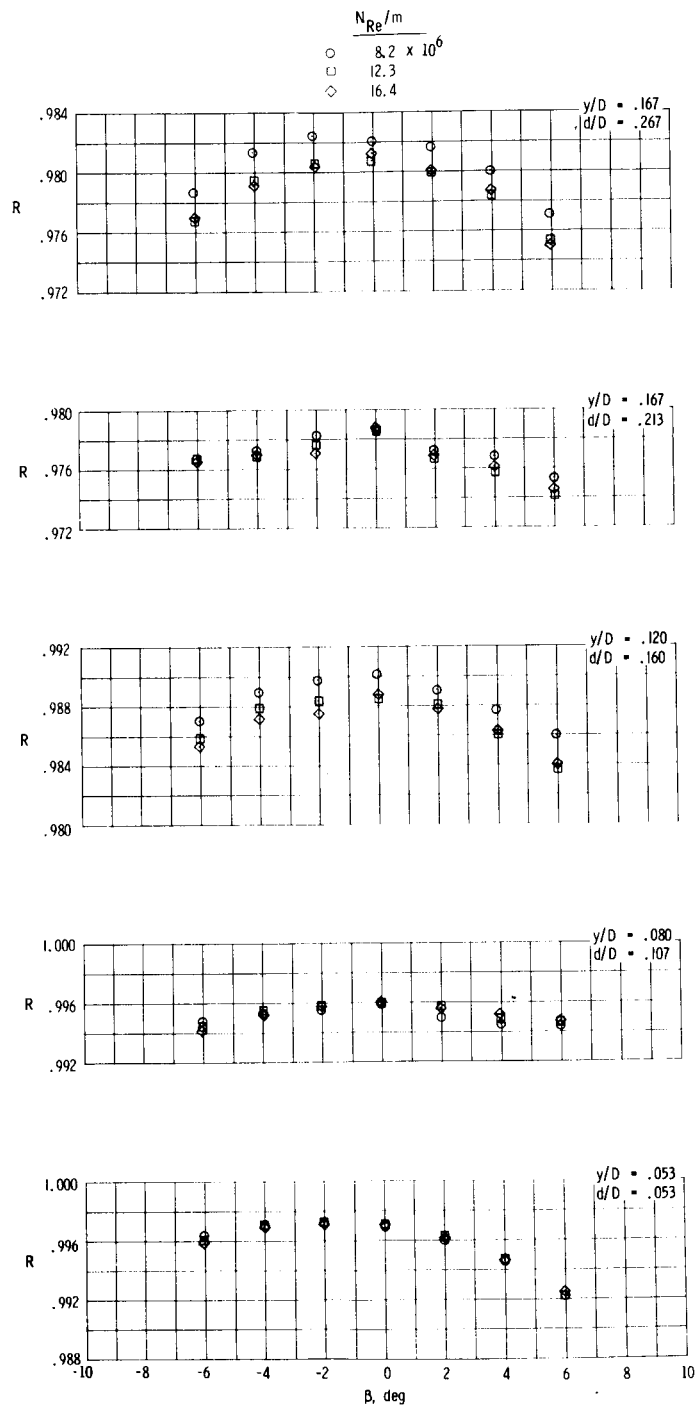
Figure 13.- Effect of variation of Reynolds number on the total-pressure recovery for each pitot-tube size over the angle-of-attack range at a Mach number of 1.83.

$r/D = 6.0$; $\beta \approx 0^\circ$.



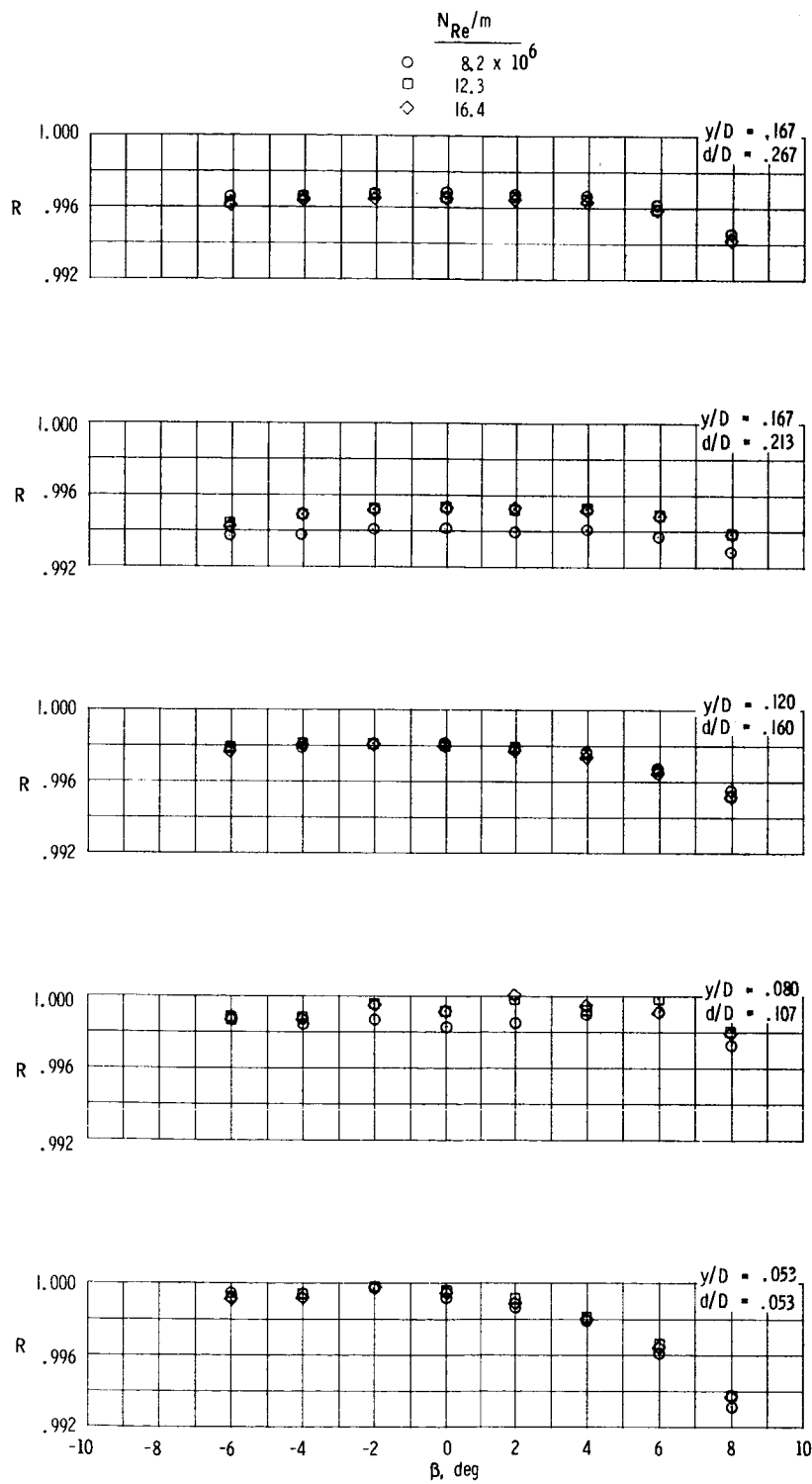
(b) $0.120 \leq y/D \leq 0.167$.

Figure 13.- Concluded.



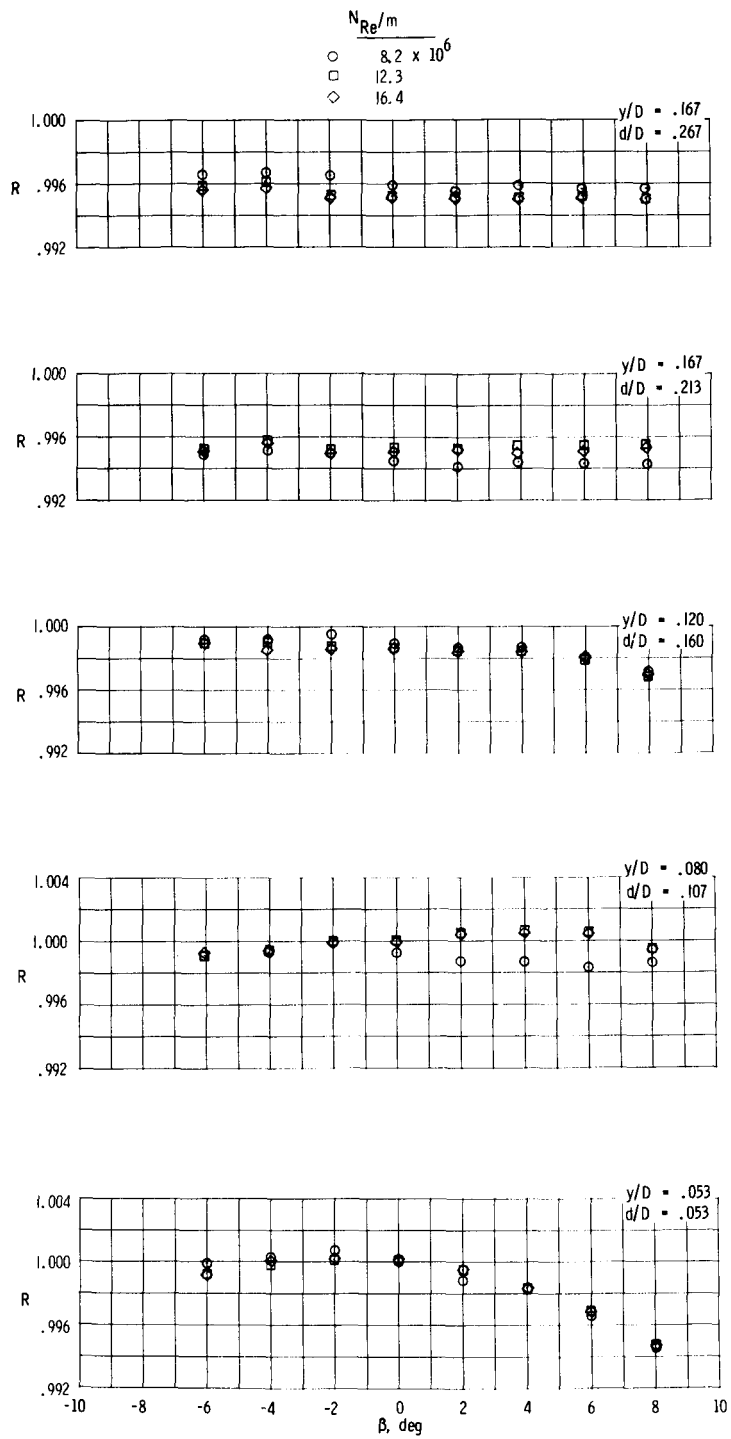
(a) $\alpha \approx -7.8^\circ$.

Figure 14.- Effect of variation in Reynolds number on the total-pressure recovery for each pitot-tube size over the angle-of-yaw range at discrete angles of attack and a Mach number of 1.83. $r/D = 6.0$.



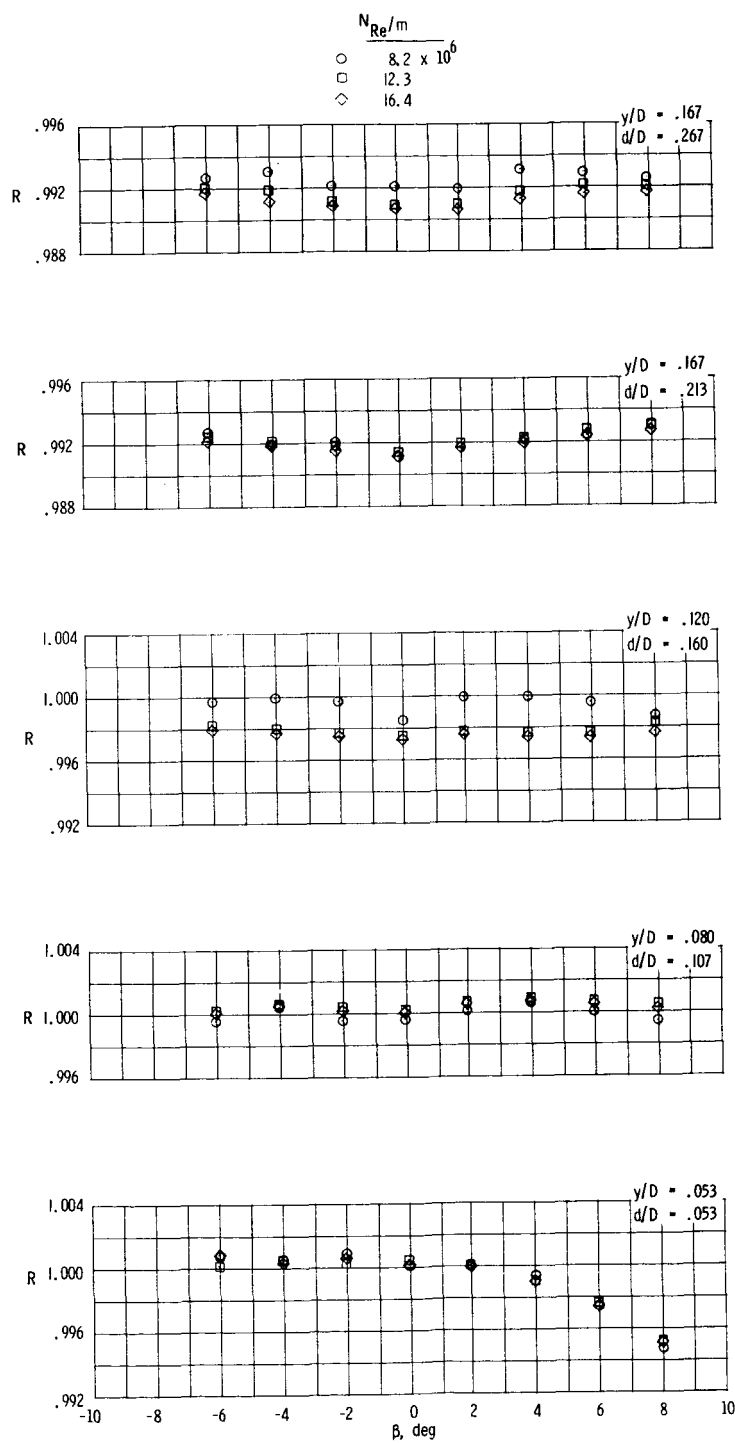
(b) $\alpha \approx 3.8^\circ$.

Figure 14.- Continued.



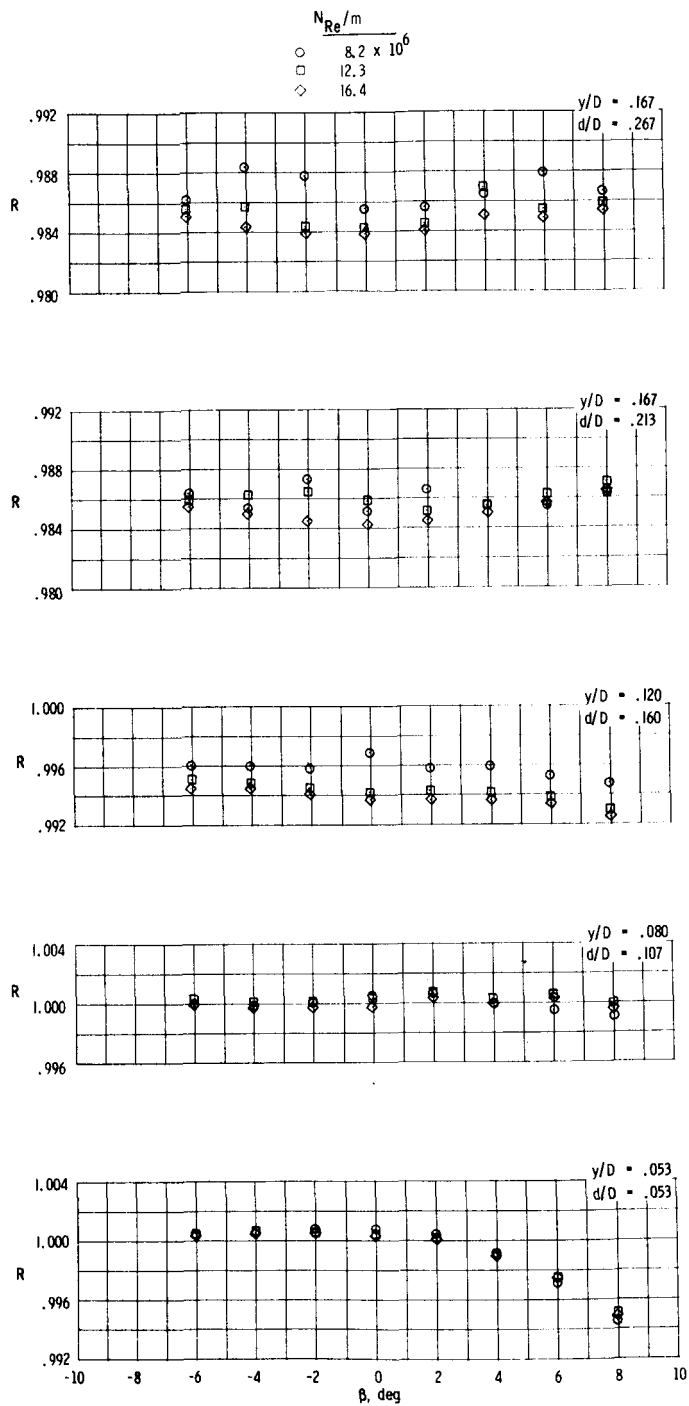
(c) $\alpha \approx 0.2^\circ$.

Figure 14.- Continued.



(d) $\alpha \approx 4.3^\circ$.

Figure 14.- Continued.



(e) $\alpha \approx 8.2^\circ$.

Figure 14.- Concluded.

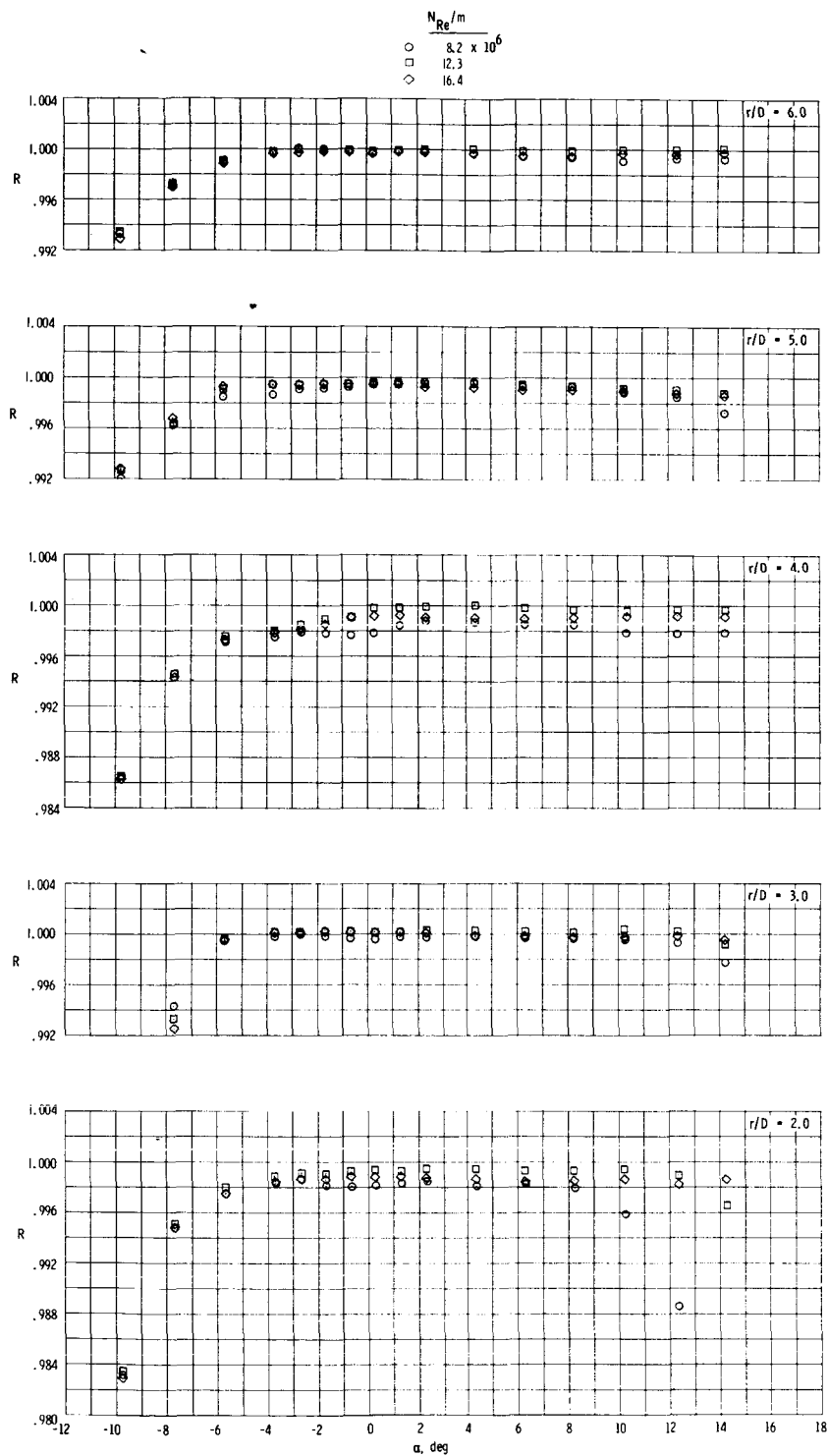
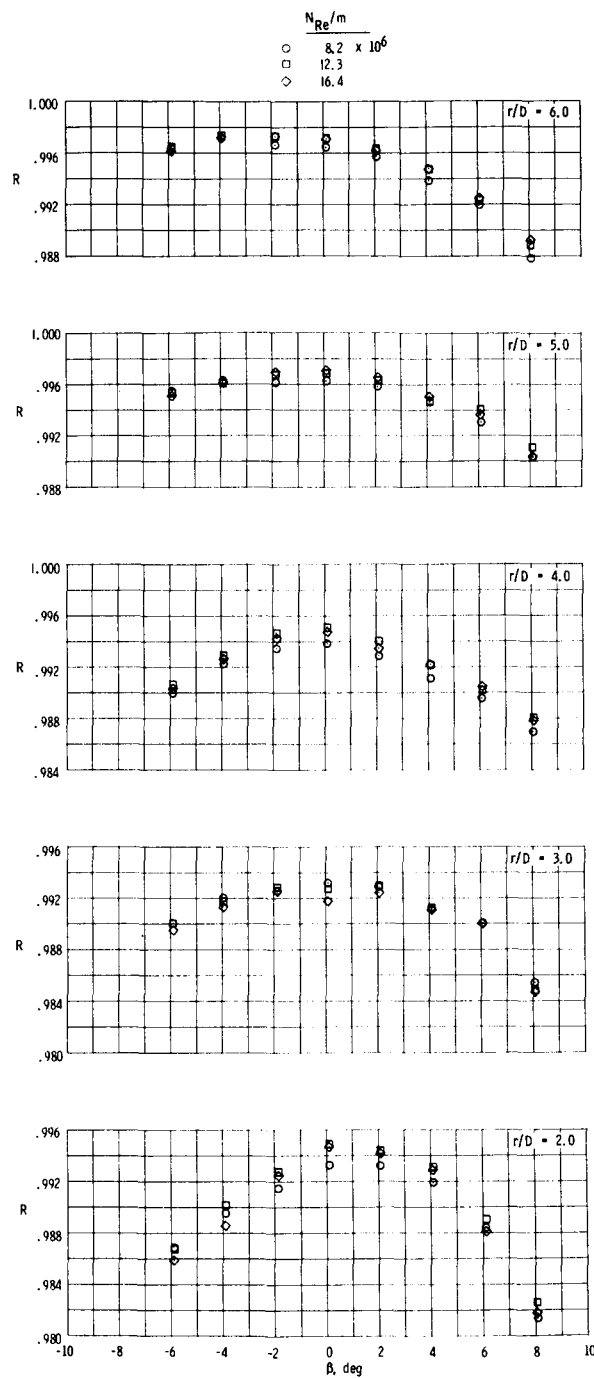
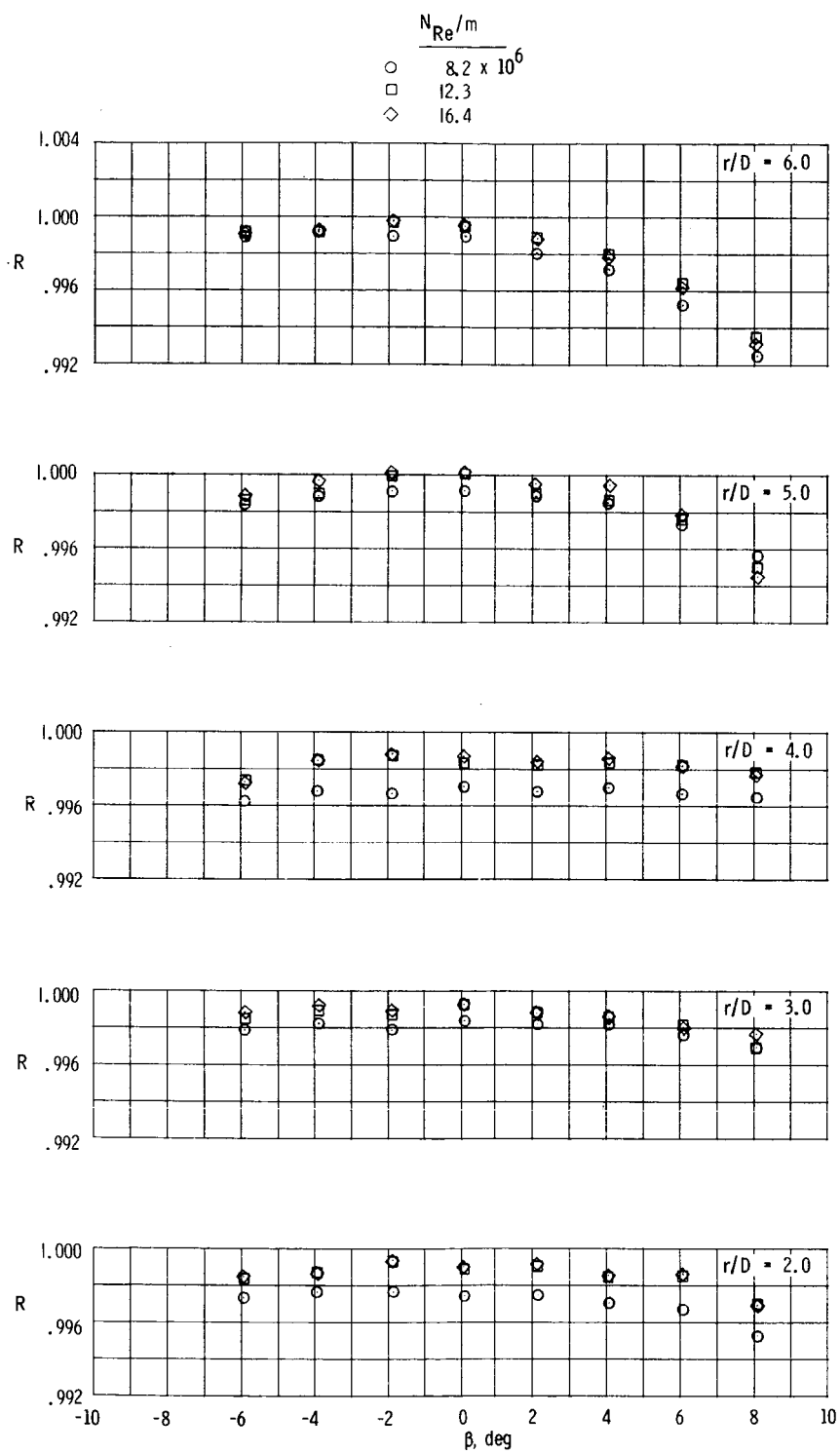


Figure 15.- Effect of variation of Reynolds number on the total-pressure recovery for each surface curvature over the angle-of-attack range at a Mach number of 1.83. $y/D = 0.053$; $\beta \approx 0^\circ$.



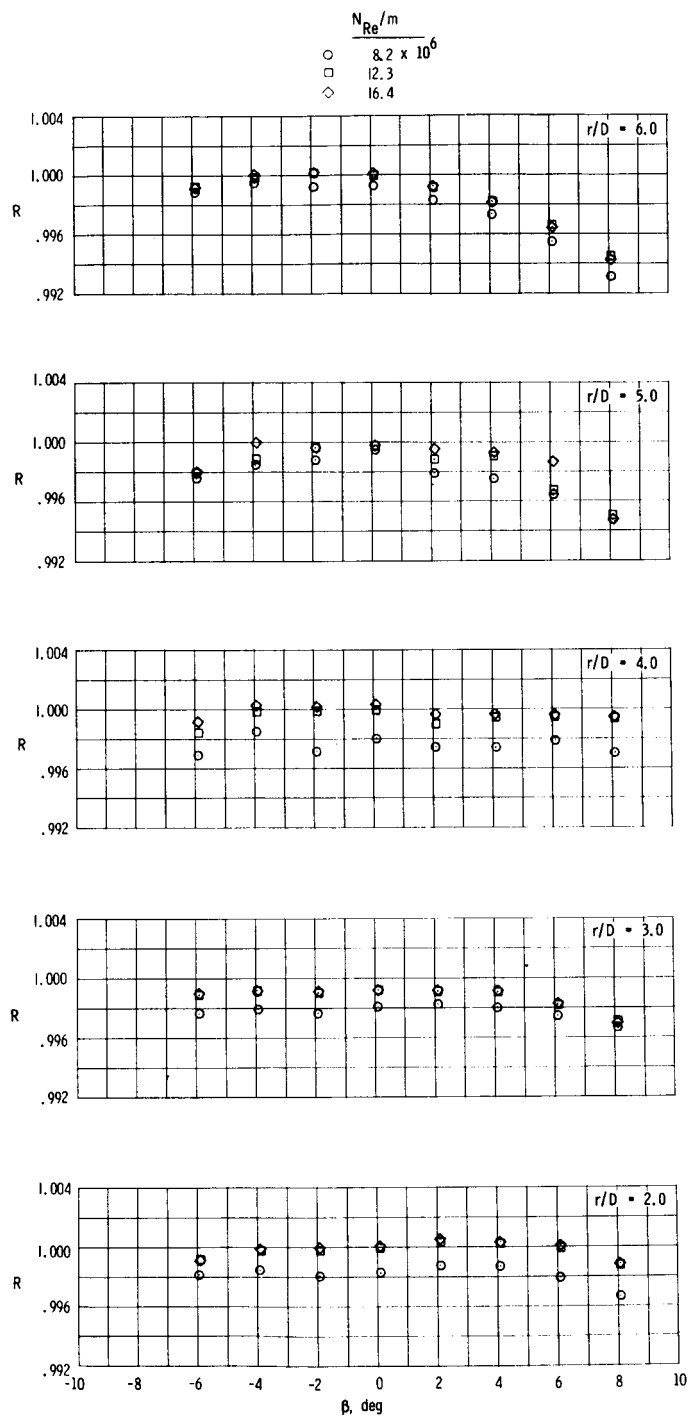
(a) $\alpha \approx -7.7^\circ$.

Figure 16.- Effect of variation of Reynolds number on the total-pressure recovery for each surface curvature over the angle-of-yaw range at discrete angles of attack and a Mach number of 1.83. $y/D = 0.053$.



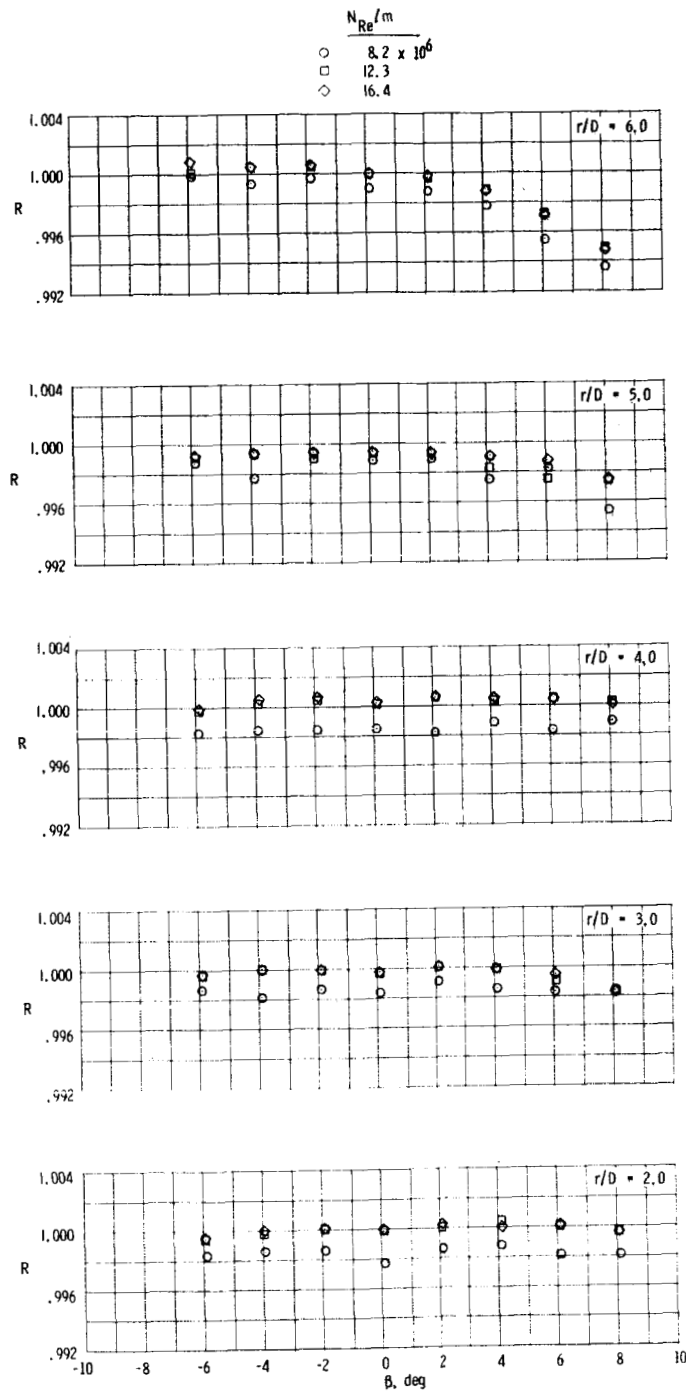
(b) $\alpha \approx -3.7^\circ$.

Figure 16.- Continued.



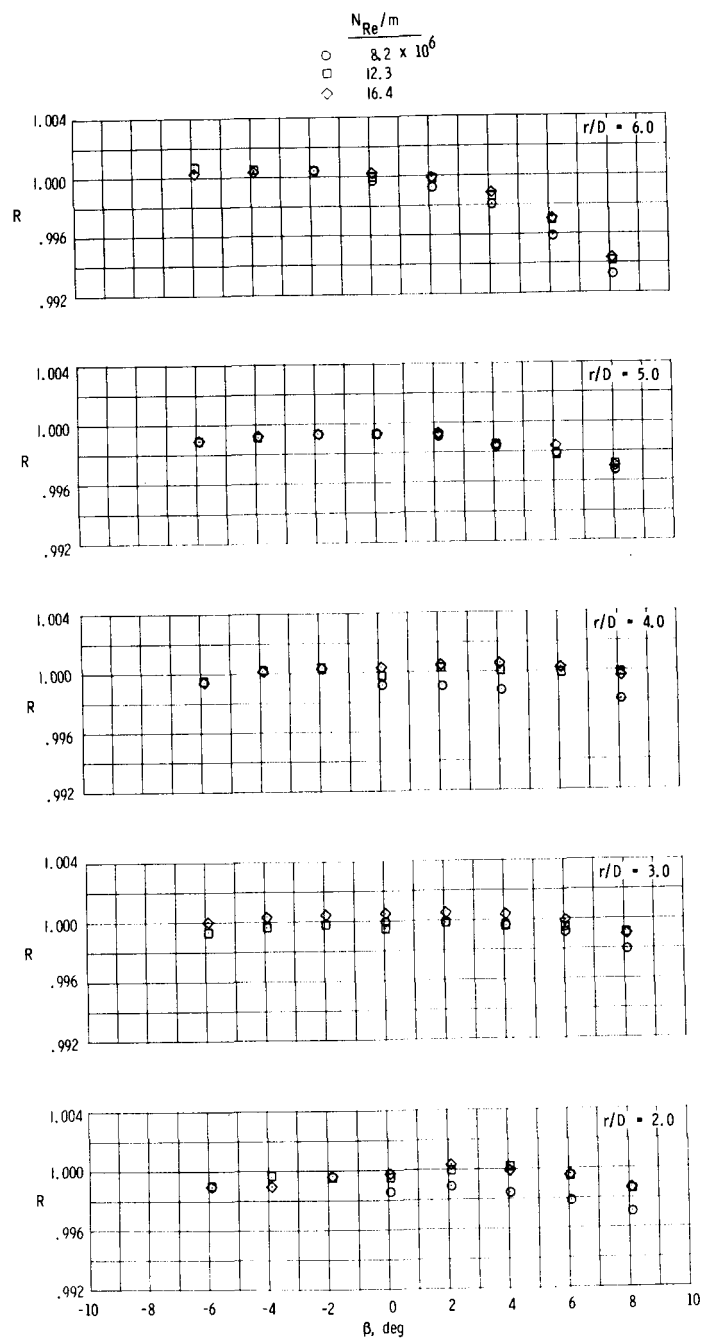
(c) $\alpha \approx 0.3^\circ$.

Figure 16.- Continued.



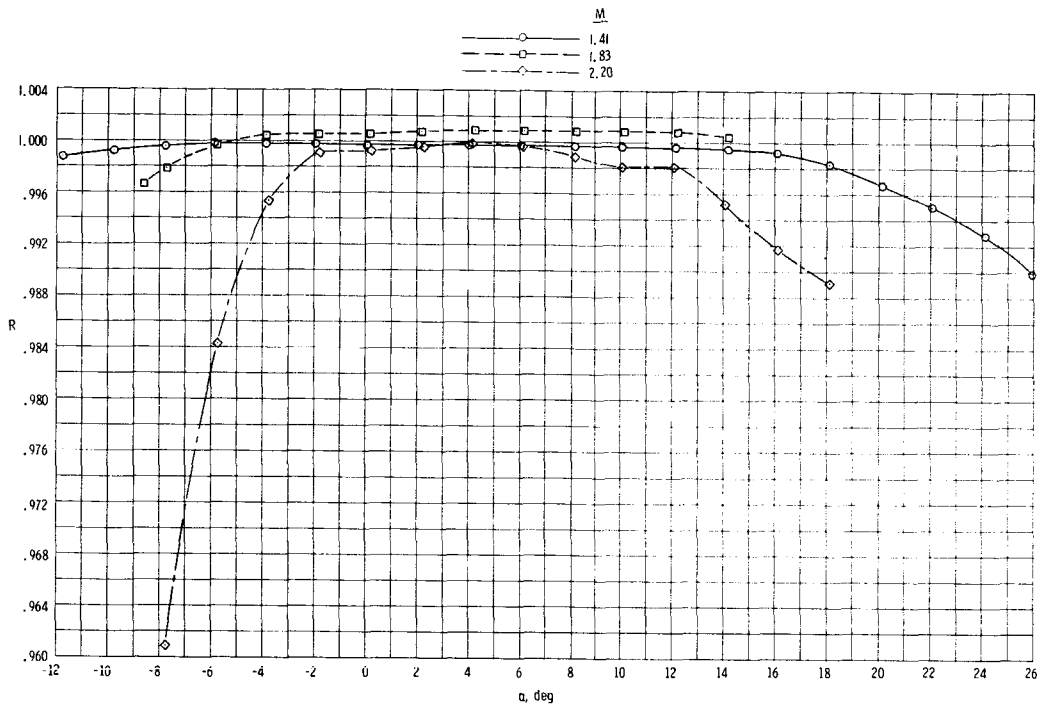
(d) $\alpha \approx 4.4^\circ$.

Figure 16.- Continued.

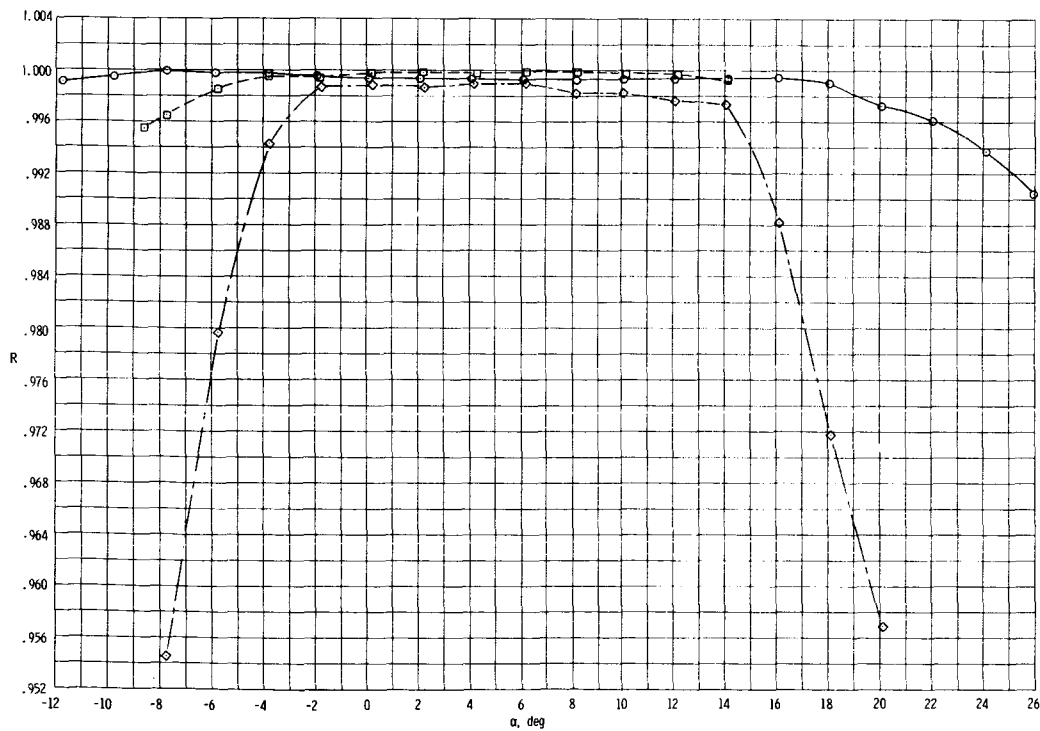


(e) $\alpha \approx 8.1^\circ$.

Figure 16.- Concluded.

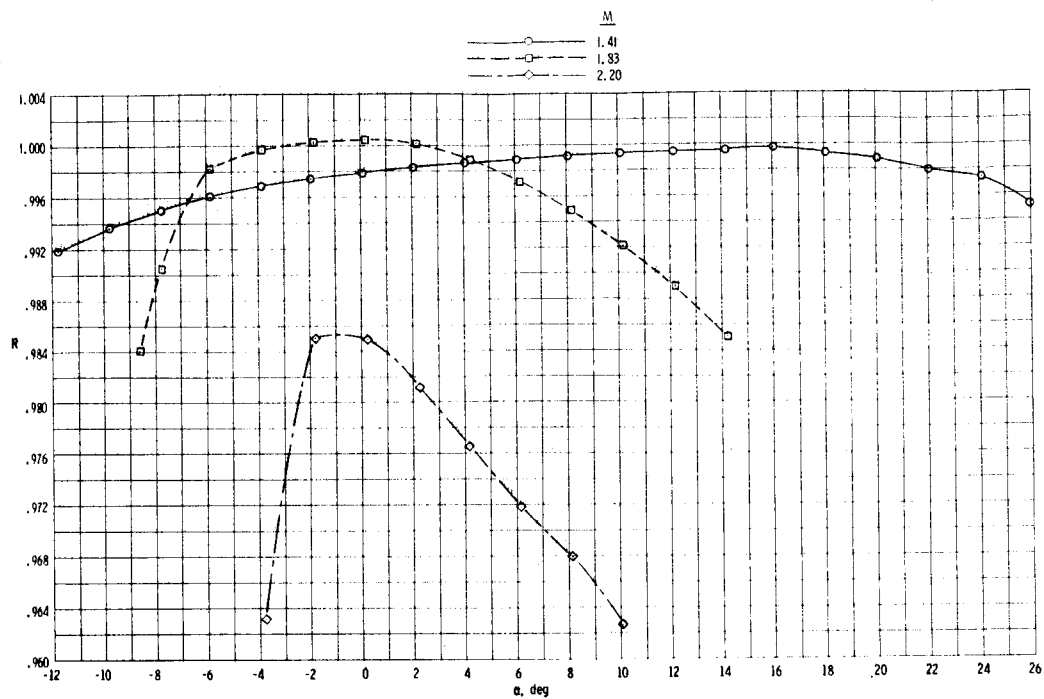


(a) $y/D = 0.053$ ($d/D = 0.053$).

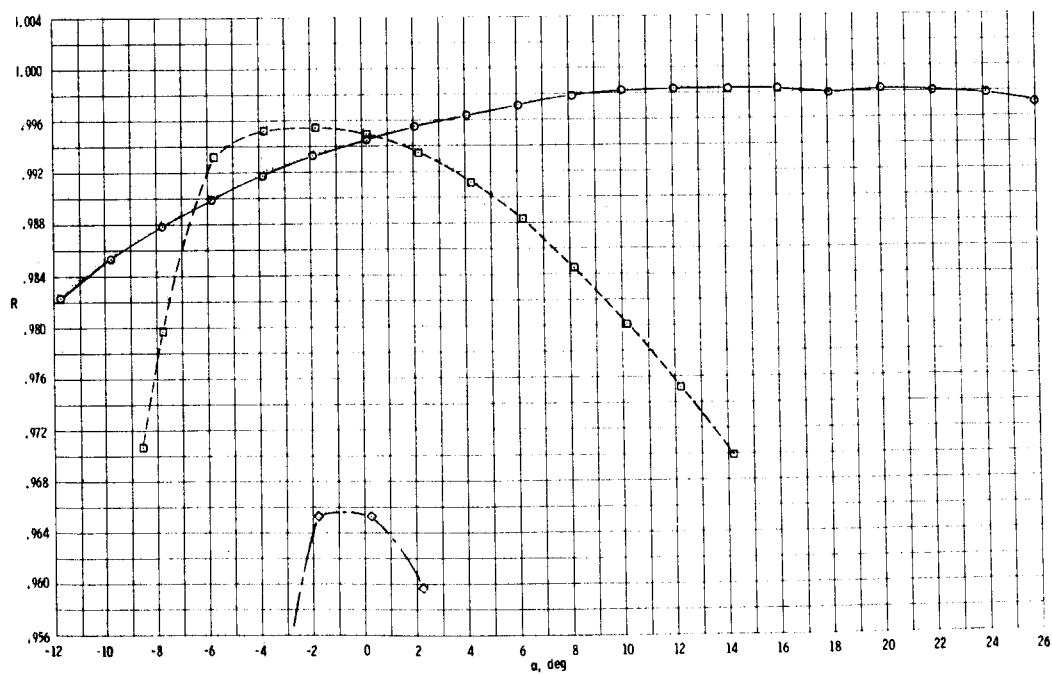


(b) $y/D = 0.080$ ($d/D = 0.107$).

Figure 17.- Effect of variation of Mach number on the total-pressure recovery for each pitot-tube size throughout the angle-of-attack range. $r/D = 6.0$; $\beta = 0^\circ$; $p_{t,1} = 103.42$ kPa.

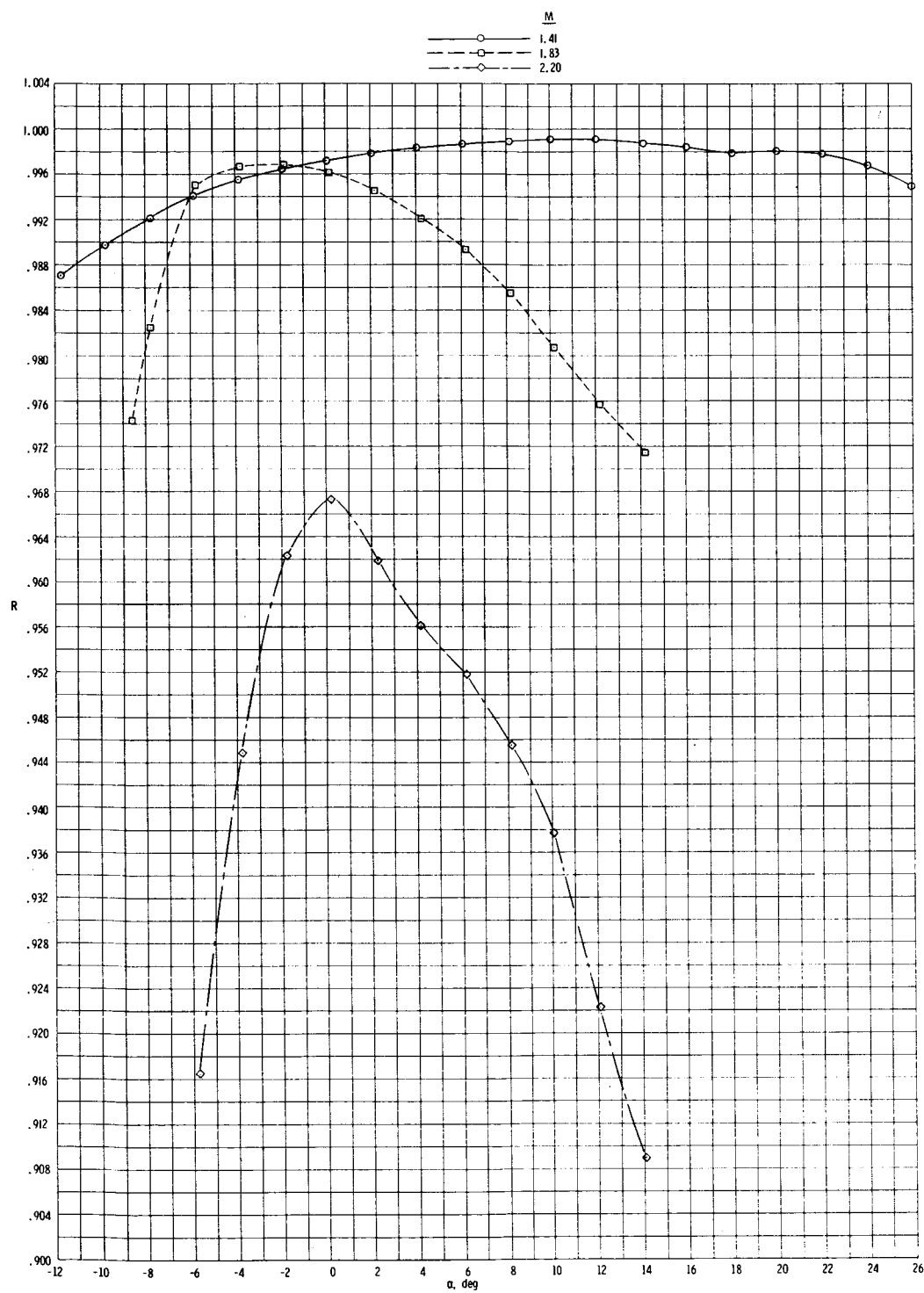


(c) $y/D = 0.120$ ($d/D = 0.160$).



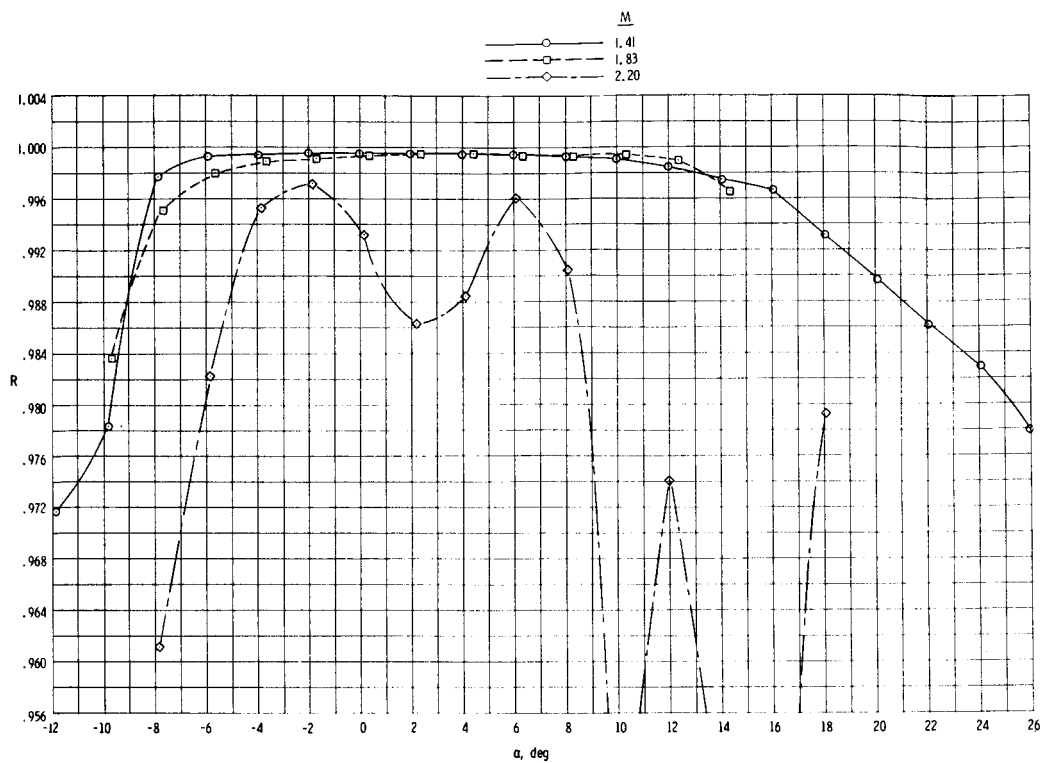
(d) $y/D = 0.167$ ($d/D = 0.213$).

Figure 17.- Continued.

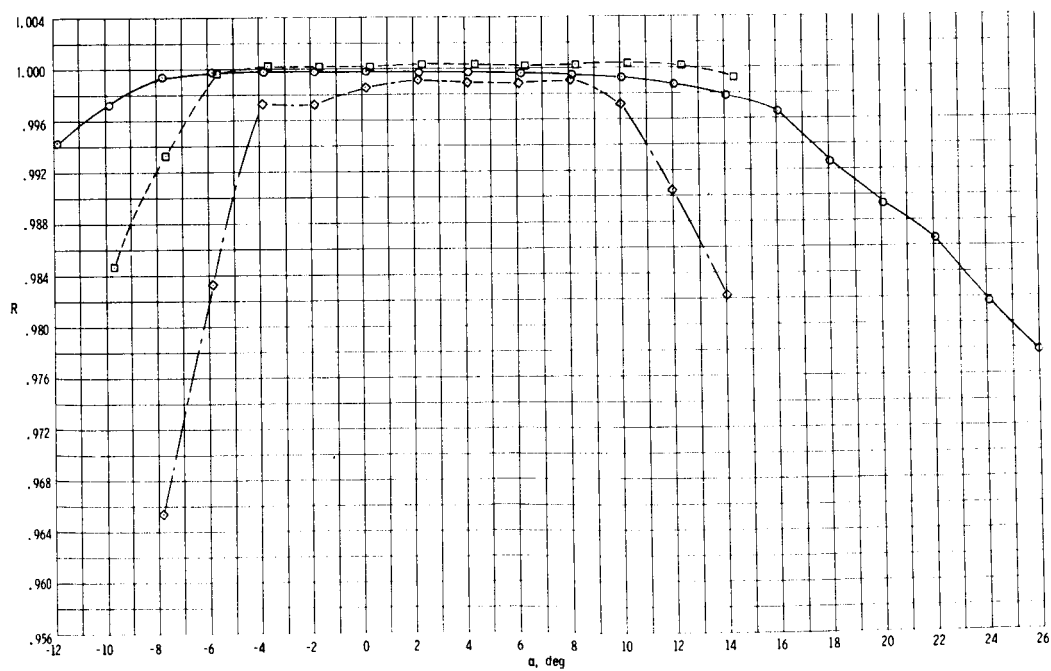


(e) $y/D = 0.167$ ($d/D = 0.267$).

Figure 17.- Concluded.

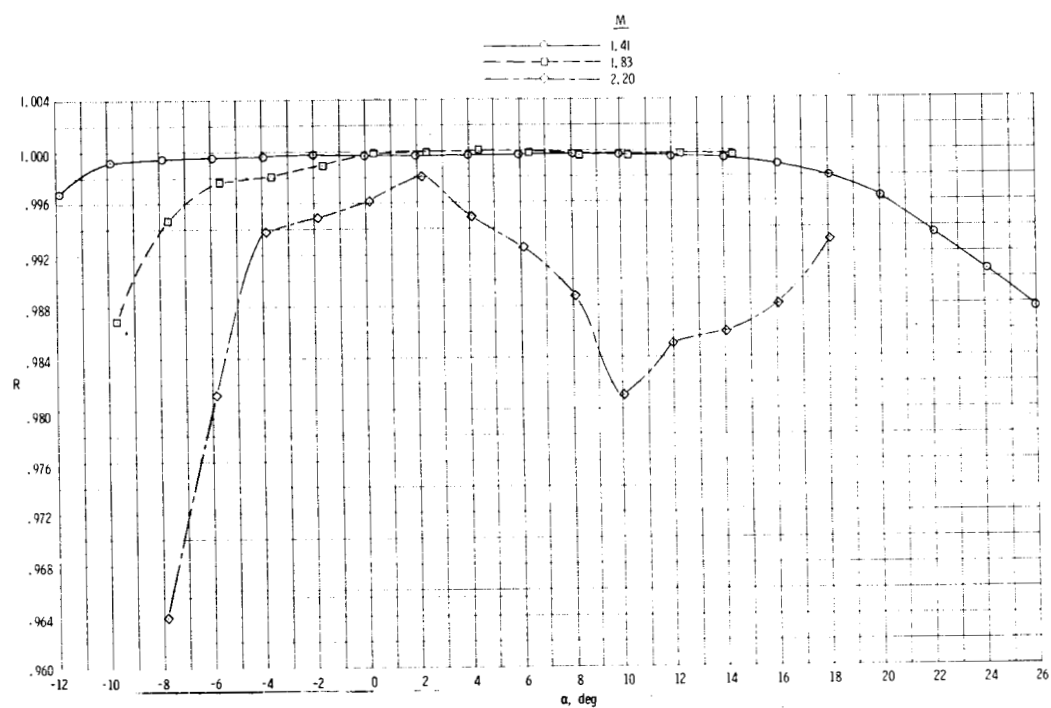


(a) $r/D = 2.0$.

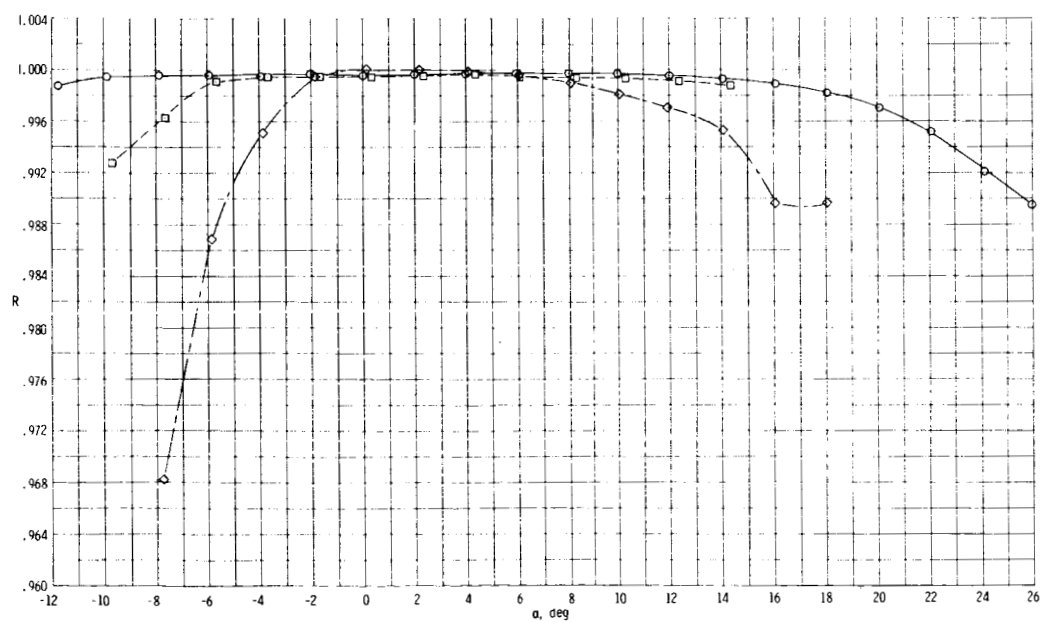


(b) $r/D = 3.0$.

Figure 18.- Effect of variation of Mach number on total-pressure recovery for each surface curvature throughout the angle-of-attack range. $y/D = 0.053$; $\beta \approx 0^\circ$; $p_{t,1} = 103.42$ kPa.

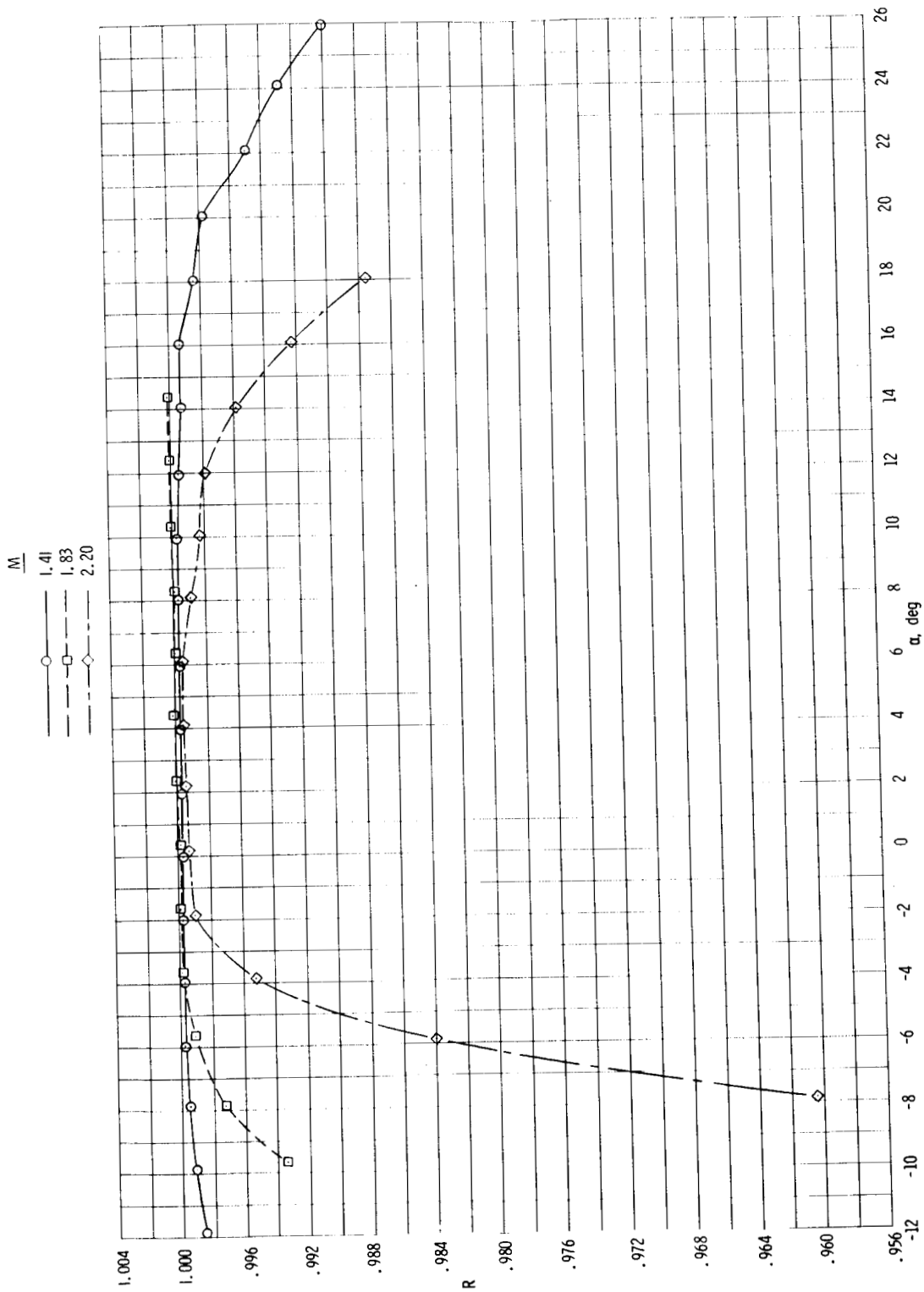


(c) $r/D = 4.0$.



(d) $r/D = 5.0$.

Figure 18.- Continued.



(e) $r/D = 6.0$.

Figure 18.- Concluded.